UNIVERSITY OF TARTU
Faculty of Science and Technology
Institute of Technology

Artur Astapenka

RNA Granules in Human Neuroblastoma Cell Line SH-SY5Y

Bachelor's Thesis (12 ECTS)

Curriculum Science and Technology

Supervisors:
Professor, PhD Arto Pulk
Professor, PhD Kalle Kipper

Tartu 2020

RNA Granules in Human Neuroblastoma Cell Line SH-SY5Y

Abstract:

We aimed to establish a protocol for the purification of neuronal RNA granules from all-trans retinoic acid differentiated human neuroblastoma cell line SH-SY5Y. Different biochemical purification methods were tested for obtaining a homogenous preparation of RNA granules for later structural analysis by cross-linking coupled mass-spectrometry or single-particle cryo-electron microscopy. The major problem encountered was a significant amount of copurifying cellular glycogen granules in the RNA granule preparations obtained by a combination of velocity sedimentation and size-exclusion chromatography. However, a majority of the contaminating glycogen could be removed from the RNA granule preparations using a maltose-binding protein (MBP) or artificial FLX protein based Ni-Sepharose or Flag-resin affinity chromatography. Besides, changes in the expression levels of mRNAs important for neuronal differentiation and synaptic function upon SH-SY5Y differentiation were analyzed. A western blot analysis revealed the presence of key RNA granule components previously identified in rat cortical RNA granules (e.g. CAPRIN-1, G3BP-1, and G3BP-2) in the SH-SY5Y derived RNA granules.

Keywords:

SH-SY5Y, neuroblastoma, RNA granules, retinoic acid, differentiation

CERCS:

Neurology, neuropsychology, neurophysiology (B640)

RNA graanulite uurimus inimese neuroblastoomi SH-SY5Y rakuliinis

Lühikokkuvõte:

Käesoleva bakalaureusetöö eesmärgiks oli välja töötada meetodid inimese luuüdikasvajast pärit SH-SY5Y rakuliini kasutamiseks *in vitro* mudelsüsteemina neuronaalsete RNA graanulite ekspressiooniks ja puhastamiseks. Töö käigus testiti erinevaid biokeemilise puhastamise meetodeid võimalikult homogeense RNA graanulite preparatsiooni valmistamiseks retinoolhappe toimel differentseeritud SH-SY5Y rakkudest hilisemaks RNA graanulite struktuuri analüüsiks ristsidumise massispektromeetria või krüo-elektronmikroskoopia abil. Peamiseks raskuseks osutus töös glükogeeni graanulite kaasapuhastumine RNA graanulitega. RNA graanulite esialgse preparaadi täiendav puhastamine maltoosi siduva valgu või tehisvalgu FLX afiinsusresinil (Ni-sefaroos või Flag,

vastavalt) võimaldas siiski kontamineerivat glükogeeni edukalt eemaldada. Töö käigus analüüsiti lisaks retinoolhappe poolt indutseeritud differentseerumisega kaasnevaid muutusi neuronaalsete mRNA-de ekspressioonitasemes SH-SY5Y rakkudes. Western blot analüüs tuvastas roti ajukoorest eraldatud RNA graanulitele omaste oluliste RNA graanuli funktsiooni regulerivate valkude nagu Caprin-1, G3BP-1 ja G3BP-2 olemasolu SH-SY5Y rakkudest eraldatud RNA graanulites.

Võtmesõnad:

SH-SY5Y, neuroblastoom, RNA graanulid, retinoolhape, differentseerumine

CERCS:

Neuroloogia, neuropsühholoogia, neurofüsioloogia (B640)

TABLE OF CONTENTS

TERMS, ABBREVIATIONS AND NOTATIONS

4E-BP – eukaryotic translation initiation factor 4E binding protein

4EGI-1 – α-[2-[4-(3,4-Dichlorophenyl)-2-thiazolyl]hydrazynylidene]-2-nitro-benzenepropanoic acid

5% milk-TBST – 5% milk powder (nonfat dried milk powder BC (AppliChem; A0830,0500)) solution in tris buffered saline with tween

aa-tRNA – aminoacyl transport ribonucleic acid

ACHE – acetylcholinesterase gene

ALX3 – homeobox protein aristaless-like 3 gene

ARM – arginine-rich motif

ATF5 – activating Transcription Factor 5 gene

ATRA – all-trans retinoic acid

BDNF – brain-derived neurotrophic factor

CDK1 – cyclin-dependent kinase 1

CHX – cycloheximide

Cis-acting element – sequence of nucleotides in messenger ribonucleic acid serving as a "localisation signal"

CMKIIα – calcium/calmodulin-dependent protein kinase type II alpha chain

CSD – cold shock domain

C_t – cycle of threshold

DLG4 – disks large homolog 4 gene

DMEM – Dulbecco′s Modified Eagle′s Medium

DMSO – dimethyl sulfoxide

dsRBD – double-stranded ribonucleic acid binding domain

EDTA – ethylenediaminetetraacetic acid

eEF1A – eukaryotic translation elongation factor 1 A

eEF2 – eukaryotic translation elongation factor 2

EGTA – ethylene glycol-bis(2-aminoethylether)-*N,N,N',N'*-tetraacetic acid

eIF1 – eukaryotic translation initiation factor 1

eIF1A – eukaryotic translation initiation factor 1 A

eIF2 – eukaryotic translation initiation factor 2

eIF3 – eukaryotic translation initiation factor 3

eIF4B – eukaryotic translation initiation factor 4 B

eIF4E – eukaryotic translation initiation factor 4 E

eIF4F – eukaryotic translation initiation factor 4 F

eIF4G – eukaryotic translation initiation factor 4 G

eIF4H – eukaryotic translation initiation factor 4 H

eIF5B – eukaryotic translation initiation factor 5 B

eIF6 – eukaryotic translation initiation factor 6

eRF1 – eukaryotic translation release factor 1

eRF3 – eukaryotic translation release factor 3

f.c. – final concentration

FBS – fetal bovine serum

FLX – artificial protein that has the flag-tag sequence at its N-terminus and ribosomal protein L9 linker helix

FMRP – fregile mental retardation protein

"full" DMEM medium – Dulbecco′s Modified Eagle′s Medium supplemented with fetal bovine serum and penicillin-streptomycin mix

“full” Neurobasal medium – Neurobasal medium supplemented with B-27, glutaMAX and penicillin-streptomycin mix

G3BP1 – Ras GTPase-activating protein-binding protein 1

G3BP2 – Ras GTPase-activating protein-binding protein 2

GAP-43 – gene encoding for neuromodulin protein

GAPDH – glyceraldehyde-3-phosphate dehydrogenase gene

GFAP – glial fibrillary acidic protein

GS – glycogen synthase

GDP – guanosine diphosphate

GTP – guanosine triphosphate

HBSS – Hank’s Balance Salt Solution

HHT – homoharringtonine

hnRNP – heterogeneous nuclear ribonucleoprotein

HOXD10 – homeobox D10 gene

iPSC – induced pluripotent stem cells

ISL1 – insulin gene enhancer gene

KCNMA1 – calcium-activated potassium channel subunit alpha-1

KH – K-homology domain

KLF13 – Kruppel like factor 13

MAP – microtubule association protein

MAP1A – microtubule association protein 1 A

MBP – maltose binding protein

mRNA – messenger ribonucleic acid

mTOR – mechanic/mammalian target of rapamycin

NCAM2 – neural cell adhesion molecule 2 gene

NCOA7 – nuclear receptor coactivator 7

NES – nuclear export signal

NeuN – neuronal nuclei gene

NFE2L2 - nuclear factor, erythroid 2 like 2 gene

NMD – nonsence-mediated decay

NMDA – n-methyl-D-aspartate

NR4A - nuclear receptor subfamily 4 group A member 1 gene

NSE – neuron-specific enolase

NT2 – N-Tera-2

NTNG2 – netrin-G2 gene

PAGE – polyacrylamide gel electrophoresis

PB – processing body

PCR – polymerase chain reaction

Pellet 1 – initial ribonucleic granules preparation obtained after the ultracentrifugation of clarified cell lysate through the sucrose cushion

Pellet 1-S500 – crude ribonucleic granules preparation obtained by size exclusion chromatography of Pellet 1 through Sephacryl S500 spin column

PMSF – phenylmethylsulfonyl fluoride

PN/STREP – penicillin-streptomycin mixture

PIC – preinitiation complex

PVDF – polyvinylidene difluoride

RBD – ribonucleic acid binding domain

RBP – ribonucleic acid binding protein

RNAg – ribonucleic acid granules

RPL7a – 60S ribosomal protein L7a

r-protein – ribosomal protein

RRM – ribonucleic acid recognition motif

rRNA – ribosomal ribonucleic acid

RT – room temperature

SDS – sodium dodecyl sulfate

SG – stress granule

SHANK1 – SH3 and multiple ankyrin repeat domains protein 1

SIX3 – homeobox protein SIX3

Stau – double-stranded RNA-binding protein Staufen homolog 1

SV2 – synaptic vesicle glycoprotein 2A

SYN1 – synapsin-1 gene

TBST – tris-buffered saline Tween-20

TCEP – tris(2-carboxyethyl)phosphine

TFAP2B – transcription factor AP-2-beta

TLX2 – T-cell leukemia homeobox protein 2

T_m – primer melting temperature

TRIS - tris(hydroxymethyl)aminomethane

tRNA – transport ribonucleic acid

UPF1 – regulator of nonsense transcripts 1

UTR – untranslated region

Znf – zinc fingers

ZNRF1 – E3 ubiquitin-protein ligase ZNRF1

INTRODUCTION

Our study focuses on the implementation of the SH-SY5Y human neuroblastoma cell line as a model system for the study of the structure and function of neuronal RNA granules. transported to and stored in dendrites and axons for a localized translation of synapse-specific mRNAs upon synaptic stimulation. Due to their role in localised translation, RNA granules are known to participate in the mechanisms of synaptic plasticity, long-term potentiation and memory formation (Kiebler and Bassell, 2006; Krichevsky and Kosik, 2001; Nakayama *et al.*, 2017). Impairments in RNA granule formation or functioning have been related to the pathogenesis of various neurodegenerative diseases (Ravanidis *et al.*, 2018). Currently, the most widely used system for the study of biochemistry and physiology of neuronal RNA granules are primary rodent-derived neuronal cultures. However, due to the technical difficulties of studying and extracting RNA granules from live animals as well as the associated ethical concerns, there is a need for establishing a more tractable *in vitro* model system for the RNA granule analysis.

Therefore, we have tried to establish the human neuroblastoma cell line SH-SY5Y as an *in vitro* model system for the purification of neuronal RNA granules. Upon application of various differentiating agents, the SH-SY5Y cell line is known to differentiate into neuronal-like cells and thus has been used as an *in vitro* model system for the study of various neurodegenerative diseases.

In this study, different biochemical purification methods were tested for the purification of RNA granules from all-trans-retinoic (ATRA) acid differentiated SH-SY5Y cells. Though a combination of velocity sedimentation and size-exclusion chromatography was able to separate the RNA granules from 80S monosomes and smaller polyribosomes, the RNA granule preparations were significantly contaminated with cellular glycogen granules whose upregulated formation is well known to be characteristic for cancer cells (Zois *et al.*, 2014). Since the failure of velocity sedimentation and size-exclusion chromatography, to remove the glycogen granules, we investigated the efficiency of different purification methods for glycogen removal. The glycogen contamination could indeed be removed when the velocity-sedimentation plus size-exclusion purified RNA granules were further purified with either maltose-binding protein (MBP) or FLX based Ni- or Flag-based affinity resin.

Removal of glycogen granules revealed the contamination of the sample with larger polysomes. Since RNA granules contain stalled polysomes as their core (Anderson and Kedersha, 2006), we did not attempt to implement any further purification procedures but rather tried the treatment of the cells with chemicals known to disrupt the translational complex formation.

Though the differentiation of SH-SY5Y with ATRA is well described in the literature, we additionally validated our differentiation protocol by monitoring the changes in the expression levels of key neuronal mRNAs tested during SH-SY5Y differentiation by previous researchers (Korecka *et al.*, 2013; Forster *et al.*, 2016).

The quality and similarity of RNA granules obtained from retinoic acid differentiated SH-SY5Y was verified by western blot comparison with rat brain-derived material among 4 key proteins known to be a part of the RNA granule.

1 LITERATURE REVIEW

1.1 Translation Mechanism in Eukaryotes

Synthesis of proteins in the cell is carried out by ribosomes – membraneless organelles consisting of two subunits: small and large (40S and 60S in eukaryotes) (Lodish *et al.*, 2008). The subunits, in turn, are composed of ribosomal RNA (rRNA) and r-proteins (Lodish *et al.*, 2008). Ribosomal protein synthesis is divided into three stages: initiation, elongation and termination. During translation initiation, two ribosomal subunits assemble into the functional 80S ribosome capable of protein synthesis guided by messenger RNA (mRNA) (Lodish *et al.*, 2008). The coding region on mRNA carries information about amino acids to be incorporated in the polypeptide chain in the form of nucleotide triplets (codons) (Lodish *et al.*, 2008). To decode the genetic information, the transport RNA (tRNA) is required. Each possible combination of three nucleotides in mRNA has a corresponding complementary anticodon in tRNA (Lodish *et al.*, 2008). Several triplets encode for a start (AUG) or stop codons (UAG, UAA or UGA) (Lodish *et al.*, 2008). Amino acids that are loaded into the ribosome are covalently attached to tRNA's 3'CCA end. During the translation, ribosome decodes the information of mRNA by monitoring mRNA-tRNA codon-anticodon coupling in the 40S subunit decoding centre, and the protein synthesis takes place in 60S subunit peptidyl transferase centre (PTC) (Lodish *et al.*, 2008). The polypeptide chain itself is synthesised starting from N-terminus and finishing with C-terminus (Lodish *et al.*, 2008). The amino acid sequence dovetails the sequence of the nucleotides in mRNA. In the process of translation, ribosomes move along mRNA in 5'-3'direction in steps of 3 nucleotides, which reflects the codon structure (Lodish *et al.*, 2008). Several ribosomes may translate single mRNA simultaneously forming the polysome (Lodish *et al.*, 2008).

The three vital steps of translation are initiation, elongation and termination. Translation initiation starts with eIF4F complex formation on mRNA and subsequent association of ribosomal subunits into 80S ribosome (Jackson *et al.*, 2010). Consequent to the translation termination, 80S ribosome is recycled and disassembled (Jackson *et al.*, 2010). Translation initiation process involves the attachment of many translation initiation factors, such as eIF1, eIF1A and eIF3 to 40S subunit (Jackson *et al.*, 2010). Subsequent binding of eIF2–GTP–Met-tRNAiMet ternary complex forms the 43S preinitiation complex (PIC) capable of association with mRNA (Jackson *et al.*, 2010). Translation initiation starts with eIF4F, eIF4B and eIF4H unwinding the 5' cap region of mRNA, making the attachment of 43S complex possible (Jackson *et al.*, 2010). 5' cap is the guanine nucleotide at the very 5' end of the

mRNA that is connected to the mRNA via 5'-5' triphosphate linkage and having the methylated guanosine on the 7th position (Banerjee, 1980). 5' cap prevents the mRNA from exonuclease degradation (Furuichi *et al.*, 1977) and facilitates its nuclear export (Lewis and Izaurralde, 1997). Upon unwinding the cap, an integral part of eIF4F – eIF4G – recruits eIF3 that is bound to small ribosomal subunit (Jackson *et al*., 2010). After association with 5'cap, 48S PIC is formed that moves along 5' untranslated region (5'UTR), scanning the mRNA for the start codon (Jackson *et al.*, 2010). The AUG start codon must bear the location in a proper context: -3 nucleotide must be purine and +4 – guanine (Jackson *et al*., 2010). Once the start codon is recognised, eIF1A becomes tighter attached to the 40S subunit, and eIF1 dissociates from the complex (Jackson *et al*., 2010). These events switch the complex to the "closed" state, locking it on the mRNA (Jackson *et al.*, 2010). Joining of two ribosomal subunits and dissociation of initiation factors happens at the same time and is mediated by the activity of eIF5B and eIF6 (Jackson *et al*., 2010).

Ribosome contains three canonical tRNA binding sites: E, P and A (Lodish *et al*., 2008), but during translation tRNA's can also adopt hybrid states. At the start of the elongation step of translation, AUG codon is located in the P-site of the ribosome, and the next codon – in the A-site (Dever *et al*., 2018). eEF1A-GTP-aminoacyl-tRNA with the corresponding anticodon binds into hybrid A/T-site and subsequently into the A-site (Dever *et al*., 2018). This binding triggers the dephosphorylation of GTP by eEF1A, and subsequent translocation of eEF1A-GDP, leading to the rapid formation of a peptide bond between peptidyl-tRNA in the P-site and aminoacyl-tRNA (aa-tRNA) in A-site (Dever *et al*., 2018). Upon the formation of the bond, the polypeptide is transferred from peptidyl-tRNA to the amino group of aa-tRNA (Dever *et al*., 2018). eEF2 binds to the A-site releasing the codon-anticodon paring and allowing for the translocation of tRNAs (Dever *et al*., 2018). The processes of tRNAs translocation and ribosomal movement are accompanied with the rotation of the ribosomal subunits relatively to each other (Dever *et al*., 2018). Release of the deacylated tRNA from E-site is coupled with the binding of the aa-tRNA to the A-site, finishing the cycle (Dever *et al*., 2018).

Translation termination takes place once a stop codon (UAA, UGA, UAG) enters the A-site of the ribosome (Dever and Green, 2012). eRF1 is a protein with the shape resembling the tRNA (Dever and Green, 2012). eRF1 occupies A-site upon reaching the stop codon and hydrolyses the peptidyl-tRNA with the help of GTPase activity of eRF3 (Dever and Green, 2012). Bound eRF1:eRF3 ensures intrinsic conditions for the separation of subunits (Dever

and Green, 2012). The process is relatively slow unless facilitated by ATPase ABCE1, which is apparent to convert chemical energy into the mechanical one required for the separation (Dever and Green, 2012).

1.2 RNA Granules in Eukaryotic Cells

Process of translation is not so straight forward in real life and can involve much more steps and mechanisms. Due to the requirement for the localised translation of mRNAs and during stress, mRNAs can associate into membraneless granules (Bramham and Wells, 2007). There are three main types of RNA granules (RNAgs) found in the cell: stress granules (SGs), processing bodies (PBs) and transport RNA granules (Bramham and Wells, 2007). First two types are only present when stress conditions are applied, the latter one is the type of RNAg's used for transportation purposes (Bramham and Wells, 2007). Transport RNA granules make up most of the RNAg's under the normal conditions, thus, they show a wide diversity of the composition and structure (Bramham and Wells, 2007).

Upon stress conditions, the number of stalled PICs in the cell increases, and these complexes tend to aggregate into SGs (Panas *et al.*, 2016). SGs participate in the pathogenesis of cancer, neurodegeneration, viral infections etc (Panas *et al.*, 2016). The number of SGs is dependent on the translational activity of mRNAs: an increase in the rate of mRNA translation suppresses the formation of SGs and vice versa (Panas *et al.*, 2016). Two main mechanisms are explaining such correlation: mechanic/mammalian target of rapamycin (mTOR) and eIF2 dependent (Panas *et al.*, 2016). mTOR is an enzyme that phosphorylates eIF4E binding protein (4E-BP), but during the metabolic stress, the mechanism misfunctions, leading to the creation of eIF4E:4E-BP complexes (Panas *et al.*, 2016). 4E-BP bound eIF4E cannot present its usual function to circulate the mRNA by binding to the 5' cap structure and joining it with the poly-A tail (Panas *et al.*, 2016). The eIF2 dependent mechanism is comprised of phosphorylation of eIF2α by stress-sensing serine/threonine kinases that disable GTPase activity of eIF2, preventing the delivery of Met-$tRNA_i^{Met}$, thus, disrupting PIC formation and further association of the 60S ribosomal subunit (Panas *et al.*, 2016). Both mechanisms lead to the failure of translation initiation and the formation of abnormal stalled PICs which in turn facilitates the SGs assembly (Panas *et al.*, 2016). SGs are comprised of a core – RNA and stalled PIC – and associated proteins binding to the core directly or attaching to other proteins (Panas *et al.*, 2016). Presence of untranslated mRNAs is crucial for SG formation, thus, polysome stabilising antibiotics such as cycloheximide suppresses the SG assembly (Panas *et al.*, 2016). SGs are involved in various signalling pathways, and their composition

differs per the cell type and stress applied (Panas *et al.*, 2016). One of the key proteins in the SGs formation process is G3BP which promotes the SG assembly by forming multimers (Matsuki *et al.*, 2012). G3BP mediates the interactions between SG and PB, promoting the preservation of polyadenylated mRNAs (Aulas *et al.*, 2015)

Processing bodies are spheroid particles containing components of nonsense-mediated decay mechanism (NMD), 5'-3' RNA decay machinery and RNA-induced silencing complex (Anderson and Kedersha, 2006). PBs are the sites for the degradation of RNAs, and they interact with SGs in the stressed cells. PBs and SGs have a similar structure, but the assembly of PBs does not require phosphorylation of eIF2α, and the exact mechanism remains unclear (Anderson and Kedersha, 2006).

Transport RNA granule is a distinct type of RNAg's devoted to the transportation of translationally repressed mRNAs (Kiebler and Bassell, 2006). Most of the protein synthesis in neurons takes place in the soma of the cell (Fatimy *et al.*, 2016). However, localised translation is crucial for the synaptic plasticity, polarisation and plays a role in the memory formation and learning process (Kiebler and Bassell, 2006). Thus, to ensure the proper and quick response, local pool of mRNAs has to be maintained in presynaptic axonal terminals and postsynaptic dendritic spines (Fatimy *et al*., 2016). Transport RNA granules are capable of bidirectional transport and most likely translocate with the help of motor proteins such as kinesin and dynein (Kiebler and Bassell, 2006). These structures, unlike SGs, contain both ribosomal subunits, elongation factors and RBPs which reflects their function of the rapid start of the translation once it is necessary (Anderson and Kedersha, 2006). Next two subsections will describe transport RNA granules in more detail.

1.3 RBP's and mRNA's of Neuronal Transport RNA Granules

Considering the unique properties of neural cells and their organisation, such processes as localised translation and mRNA transport to neurites are crucial for the proper functioning of neurons (Ravanidis *et al.*, 2018). These processes occur under mediation by RBPs that compose a significant part of the transport RNA granule (Ravanidis *et al.*, 2018). A considerable cohort of these proteins is restricted to the brain exclusively, and each can recognise the structural motifs or nucleotide sequences of target mRNAs (Ravanidis *et al.*, 2018). Two of the most common RBPs involved in the formation of transport RNA granules are Stauften (Stau) and Fragile-X Mental Retardation Protein (FMRP) (Ravanidis *et al.*, 2018). Dysfunction of both of these proteins leads to developmental delay, decreased mental

capacity and abnormal morphology of dendritic spines (Ravanidis *et al.*, 2018). Stau and FMRP colocalise with transport RNA granules during their transport, thus, participating in the process (Ravanidis *et al.*, 2018). Besides, FMRP suppresses translation by promoting stalling of ribosomes and enlarging the granules (Ravanidis *et al.*, 2018). Two other important RBPs are CAPRIN-1 and G3BP. CAPRIN-1 is crucial for the dendritic localisation of transport RNA granules, and CAPRIN-1 knock out mice shows a significant impairment in the dendritic mRNA transport process and long-term memory formation (Nakayama *et al.*, 2017). G3BP1 was historically associated with SG formation (Matsuki *et al.*, 2012) and interaction with PB (Aulas *et al.*, 2015). However, recent findings suggest non-canonical role of G3BP1 or G3BP2 as an enhancer of mRNA stability (Laver *et al.*, 2020) and it's colocalisation with mRNAs in axons without any stress (Sahoo *et al.*, 2018). Such reports give grounds for the suggestion that G3BP is present within transport RNA granules.

Using deep sequencing and fluorescent labelling approaches, 2550 mRNAs that localise in neurites and have three orders higher abundance there than in soma were identified (Cajigas *et al.*, 2012). These transcripts encode for the proteins crucial for synapsis operation and proper neurite development (Cajigas *et al.*, 2012). The most abundant mRNA discovered encodes for CMKIIα protein which directly organises and regulates the Ca^{2+} signalling and plays a significant role in long-term potentiation and spatial learning (Cajigas *et al.*, 2012. Other mRNAs found in considerable numbers are SHANK1, DLG4 and MAP1A (Cajigas *et al.*, 2012. Deletion in the SHANK1 gene causes autism in male mice, and the protein is critical for the normal development and function of synapses. DLG4 serves as a scaffold protein for the clustering of receptors, ion channels and signalling proteins. MAP1A protein forms microtubules vital for the cytoskeleton of neurites and neurogenesis process. The data on the genes was retrieved from NCBI Genbank database.

mRNAs possess cis-acting elements that serve as "localisation elements" in the molecular machinery of the cell to ensure the proper localization (Di Liegro *et al.*, 2014). Cis-acting elements, having a variable length from several to a hundred nucleotides, mainly locate in the 3'UTR, but can also be found in the 5'UTR and coding regions (Martin and Ephrussi, 2009). However, identification of these cis-acting elements is not always straightforward as their activity can be context-dependent which is associated with certain difficulties in the research as controversial results for several mRNAs have been obtained (Martin and

Ephrussi, 2009). Interaction between RBPs and mRNAs is mediated by RNA-binding domains (RBDs) of restricted variability (Ravanidis *et al.*, 2018). Six most abundant types of RBDs are RNA recognition motif (RRM), heterogeneous nuclear ribonucleoprotein (hnRNP) K-homology domain (KH), zinc finger domain (Znf), cold-shock domain (CSD), arginine-rich motif (ARM) and double-stranded RNA binding domain (dsRBD) (Ravanidis *et al.*, 2018). Fidelity in recognition of the mRNA is achieved by combining several RBDs in one RBP, even though, one mRNA may recruit several RBPs, thus, forming a transport RNA granule (Ravanidis *et al.*, 2018).

RBPs bound to the transcript determine its fate (Di Liegro *et al.*, 2014). During the transportation, transport RNA granules remain assembled, repressing the translation, unless the change in the microenvironment triggers (de)phosphorylation and methylation of RBPs, releasing the mRNA (Di Liegro *et al.*, 2014). Translation repression occurs differently depending on RBP. The most common mechanisms involve 4E-BP recruitment, direct binding to the ribosome and recruitment of deadenylase proteins that shorten the poly(A) tail of the RNA (Ravanidis *et al.*, 2018). Some RBPs contain a nuclear export signal (NES) sequences that allow for the export of the mRNA to the cytoplasm (Di Liegro *et al.*, 2014). In the cytoplasm, transport RNA granules enlarge by the attachment of additional RBPs (Martin and Ephrussi, 2009). Upon this process, the RBPs mediate the transport of transport RNA granules by the binding to the protein motors (kinesins and dyneins) either directly or via adaptor proteins (Ravanidis *et al.*, 2018). Such binding enables the usage of transport along cytoskeleton in both directions. The most well-described RBP is Stau which is evolutionary conserved for the mRNA transport as it is not only involved in the dendritic transport but also shown to contribute to the mRNA localisation in Drosophila oocytes (Ravanidis *et al.*, 2018). Mammalian Stau is composed of four RBDs that bind the RNA non-specifically (Ravanidis *et al.*, 2018).

Neural transport RNA granules show a significant degree of heterogeneity: a number of transport RNA granules contain strictly one single mRNA molecule (Batish *et al.*, 2012). Remarkably, studied mRNAs with the same cis-acting elements do not colocalise in single transport RNA granule (Batish *et al.*, 2012). The explanation for it might be the need for precise control over the transport and translation of mRNA (Batish *et al.*, 2012). Additional heterogeneity depends on the method of translation repression: translation inhibition can occur before the polyribosomes are assembled and after (Ostroff *et al.*, 2017). Prevention of the initial assembly of polyribosomes follows the cap-dependent mechanism (Ostroff *et al.*,

2017). For instance, the 4EGI-1 that interferes in eIF4E-eIF4G interactions actively participates in the process preventing the unwinding of the 5'cap (Ostroff *et al.*, 2017). Cap-dependent stalling is dominant in the heads of the dendritic spines but not in the necks and shafts (Ostroff *et al.*, 2017). Another mechanism involves stalling of already assembled polysomes. Previous studies have shown the participation of UPF1 (Graber *et al.* 2017) and FMRP in such stalling (Darnell *et al.*, 2011). UPF1 interaction with eIF3 and eRF3 prevents the release of the polypeptide, and this, in turn, halts the translation at the end of the first round (Graber *et al.* 2017). FMRP non-specifically binds to mRNA sequence and prevents the movement of ribosomes on mRNA (Darnell *et al.*, 2011). FMRP has more affinity to the coding sequence rather than to 3'UTR or 5'UTR (Darnell *et al.*, 2011). Thus, transport RNA granules show high variability that depends on such factors as the core mRNA molecule, proteins attached, mechanism of translation stalling etc.

1.4 SH-SY5Y Neuroblastoma Cell Line

Appropriate *in vitro* model is essential for the neuroscientific research. Nowadays, for the *in vitro* experiments, primary neurons and rodent cell lines are usually used. Unfortunately, this leads to the occurrence of difficulties and uncertainties. For instance, primary cell culture is hard to handle, and it stops propagation upon final differentiation (Shipley *et al*., 2016). A common concern about using both primary and secondary neuron cultures derived from rodents is a species-specific difference in metabolic processes, gene expression patterns and signalling (Shipley *et al*., 2016). Widely used in neuroscience human-derived secondary cell cultures include N-Tera-2 (NT2) and inducible pluripotent stem cells (iPSCs). However, NT2 differentiation leads to the rise of the mixture of different cells populations: neurons, astrocytes and radial glial cells – and additional purification steps are required to create the pure neuron culture (Shipley *et al*., 2016). iPSCs possess a variable karyotype which in 72% of the cells exceeds 60 chromosomes (Shipley *et al*., 2016). Moreover, their differentiation leads to populations of different degree of mature cells morphology (Shipley *et al*., 2016).

SH-SY5Y is a subline of the parental cell line SK-N-SH derived from a human metastatic bone marrow tumour biopsy and developed by Biedler group in 1970 (Shipley *et al*., 2016). The cell line consists of two distinct populations: adherent neuron-like cells and floating epithelial-like cells (Shipley *et al*., 2016). Thus, the pure culture of neuron-like cells can be obtained simply during the medium exchange when the floating cells are discarded along with it. SHSY-5Y cells have a doubling time of 27 hours (Kovalevich and Langford, 2013) and 47 chromosomes in their karyotype (Shipley *et al*., 2016). With the administration of a

variety of differentiating agents and supplementary compounds, cells can differentiate in mature cells of diverse morphology: cholinergic, adrenergic and dopaminergic – which are the main morphological groups of neurons according to their preferred neurotransmitter (Kovalevich and Langford, 2013).

The most common differentiating agent for SHSY-5Y cells is ATRA. ATRA is a derivative of vitamin A which is naturally synthesised in organisms, and it participates in the differentiation of neural cells and neurogenesis (Duester, 2008). ATRA upregulates the expression of neural markers such as growth-associated protein (GAP-43), neuronal nuclei (NeuN), synaptophysin (SYN), synaptic vesicle protein II (SV2), neuron-specific enolase (NSE) and microtubule-associated protein (MAP) (Korecka *et al.*, 2013). Moreover, glial markers such as glial fibrillary acidic protein (GFAP) show lowered expression (Korecka *et al.*, 2013). Thirteen pro-differentiation transcription factors (promoting differentiation of the cells) show an increase in expression, for example ALX3, KLF13 and NR4A (Korecka *et al.*, 2013). Six positive regulators of neural development and differentiation enhance their expression (NCOA7, TLX2, ID3, NFE2L2, ZNRF1 and HOXD10), and four negative regulators are suppressed (TFAP2B, ISL1, SIX3, ATF5) (Korecka *et al.*, 2013). Differentiated SHSY-5Y cells show neuron-like morphology with a complex extended neurite network and synapse-like connections (Kovalevich and Langford, 2013). Upon differentiation, the proliferation rate decreases, and cell cycles synchronise (Kovalevich and Langford, 2013). Higher degree of differentiation of SH-SY5Y can be obtained if ATRA treatment is followed by brain-derived neurotrophic factor (BDNF) application (Jämsä et al., 2004).

2 THE AIMS OF THE THESIS

The study is dedicated to the investigation of the possibility to implement SH-SY5Y human neuroblastoma cell line as a secondary neuron culture source of transport RNA granules. Thus, the aims stated are:

- To enable the proper source of transport RNA granules from the secondary neuron culture, we aimed to establish a protocol of SH-SY5Y culturing that would allow for the highest possible yield of transport RNA granules obtained;
- To support the statement that ATRA differentiates SH-SY5Y into neuron-like cells, we need to validate the results of the ATRA treatment;
- Find an efficient way to remove the contaminating glycogen particles from the transport RNA granule preparation;
- Prove that the neuronal granules obtained are similar to the ones in the *in vivo* system (rat brain).

3 EXPERIMENTAL PART

3.1 MATERIALS AND METHODS

3.1.1 SHSY-5Y Cell Line and Culturing

SH-SY5Y (ATCC; REF: CRL-2266) cell line stored in 5% DMSO in DMEM in the liquid nitrogen vapour phase was used for the experiments. The growth was performed at 37°C in the atmosphere of 5% CO2. The cells from the cryostock were seeded in a 10 cm diameter cell culture dish (ThermoScientific BioLite; REF: 130181; 60.8 cm^2 culturable area) to a density of 11000 cells/cm^2 in a 10 ml of Basal Cell Culture Liquid Medium – DMEM and Ham's F-12. 50/50 mix (Corning; REF. 10-090-CVR) supplemented with Regular Fetum Bovine Serum or FBS (Corning; REF. 35-015-CV) and Penicillin/Streptomycin (PN/STREP) (SIGMA; REF: P4333) mix in 100:10:1 volume ratio correspondingly ("full" DMEM). From 6 – 24 h after seeding, 100 % of initial the DMSO-containing „full" DMEM medium was replaced with 10 ml of a DMSO-free „full" DMEM medium, and the incubation continued to a 60-70% confluency. At this confluency, the cells were split to T75 flasks (Thermo Scientific BioLite 130190; 75 cm^2 culturable area) as follows. The growth medium on the cells was removed by aspiration, the cells were washed with 4 ml of a RT isotonic Hank's Balanced Salts Solution (HBSS; BioWest; REF: L0607500) and then detached from the plate by an incubation with 2 ml of Trypsin 0.25% 2.21 mM EDTA (Corning; REF. 25-053-CI) at 37°C. To inactivate the trypsin, cells were subsequently mixed with 5 volumes of „full" DMEM medium, and 5 ml of the cell suspension was added to 10 ml of „full" DMEM medium in a T75 flask. The incubation continued at 37°C until the cultures reach the confluency of 50-60%, followed by trypsinisation and splitting 3-5 ml of the cell suspension to 8 × 15 cm cell culture dishes (Thermo Scientific BioLite; REF: 130183; culturable area 148 cm^2) in a total volume of 20 mL „full" DMEM per plate. The cells were grown at 37°C to a confluency of 20-40 %, followed by a medium exchange and differentiation with ATRA as described in the following paragraph.

3.1.2 RA Differentiation of SH-SY5Y

Upon removal of 100% of "Full" DMEM medium from the cells on 8 cm culture dishes by aspirating, 15 ml of prewarmed "full" Neurobasal medium is added to each dish. "Full" Neurobasal medium contains Neurobasal medium (Gibco; REF. 21103-049), B-27 supplement (Gibco; REF. 17504-001), GlutaMAX supplement (Gibco; REF. 35050-061) and PN/STREP (SIGMA; REF: P4333) mix in the volume proportions of 100:2:1:1

correspondingly. After the initial medium addition, 5 ml of "full" Neurobasal medium with 60 μM ATRA (SIGMA; REF: 2625-100MG) are added to each dish to the final ATRA concentration of 15 μM. The cells were cultivated for 5 days at 37°C in the humid atmosphere of 5% CO_2. 50% of the growth medium is replaced with fresh "Full" Neurobasal medium containing 15 μM ATRA one day before the harvesting.

3.1.3 Cell Harvesting and Lysis for Transport RNA Granules Purification

To remove any SGs, 1 ml of 2.1 mg/ml cycloheximide (CHX; SIGMA; REF: 01810-1G) solution in "Full" Neurobasal medium was added to the cells on each culture dish to the f.c. 100 μg/ml prior to harvesting. The cells were incubated for 5 min at 37°C in the atmosphere of 5% CO_2. Following the incubation, the cells were placed on ice, and the medium was removed from the culture dishes by 25 ml sereological pipet. Th cells were twice washed with 5 ml of the ice-cold isotonic wash buffer. The wash buffer is made by adding EGTA (ethylene glycol-bis(2-aminoethylether)-*N,N,N',N'*-tetraacetic acid) to HBSS (-Ca/-Mg) to the final concentration of 0.5 mM. The cells were harvested from the dishes as follows: 2 ml of the lysis buffer (HEPES-KOH (pH7.5; f.c. 20 mM), KOAc (f.c. 10 mM), $Mg(OAc)_2$ (f.c. 4 mM), tris(2-carboxyethyl)phosphine (TCEP; f.c. 0.5 mM), CHX (f.c. 100 μg/m), Trehalose (0.35% by volume), protease inhibitor mix (ROCHE cOmplete ULTRA Tablets, Mini, EDTA-free; REF. 05 892 791001; 1 tablet per 10 ml)) were pipetted to two culture dishes, the cells were harvested using the cell scraper, and the suspensions were transferred to the next two dishes to repeat the harvest, and the resulted cell suspensions are pooled in a precooled 15 ml Falcon tube. Following components were added to the 8 ml of the collected cell suspension to the 8 ml of resulting suspension: RiboLock RNase Inhibitor (ThermoScientific; Catalogue number: EO0381; f.c. 100 U/ml), bestatin (f.c. 1 μg/ml), phenylmethylsulfonyl fluoride (PMSF; f.c. 0.1 mM), DNase I, RNase-free (ThermoScientific; Catalogue number: EN0521; f.c. 1 mU/μl) and 10% Tween 20 (f.c. 0.5% by volume). The cell lysis was performed by passing the cell suspension 3 times through a precooled gauge 26 needle. Immediately following the lysis KOAc concentration in the lysate was adjusted to 150 mM, as this concentration of monovalent ions is optimal for the structural integrity of the ribosomal complexes.

3.1.4 Transport RNA Granules Purification by Velosity Sedimentation

To obtain an transport RNA granules preparation, the KOAc-adjusted lysate was distributed between 2 ml precooled polypropylene microcentrifuge 2 ml tubes (Eppendorf; REF:

0030108132) and centrifuged in a fixed angle rotor (12084) in SIGMA 1-14K benchtop centrifuge at 2500 g/4°C for 2 min to remove nuclei. The resulting supernatant was transferred to a new 2 ml precooled tubes and subsequently centrifuged at 10625 g/4°C for 9 min. The supernatants from the second centrifugation step were pooled in a precooled polypropylene tube. If the volume of the second supernatant was lower than 8 ml, to prevent the collapse of the tube during ultracentrifugation, it's volume was brought up to 8 ml by adding 1 × SALT buffer (HEPES-KOH (pH 7.5; f.c. 20 mM), KOAc (f.c. 150 mM), $Mg(OAc)_2$ (f.c. 4 mM), TCEP (f.c. 0.5 mM), 50 µg/mL CHX) containing CHX (0.1 mg/ml) . The combined supernatant is layered on the top of 2 ml 60% sucrose cushion (68% sucrose, 10 × SALT, 0.5 mM TCEP, CHX (f.c. 50 µg/ml)) in SW41 ultracentrifuge tube. The material was centrifuged in a SW41 Ti swing-out rotor in an Optima XE-90 Ultracentrifuge (Beckman Coulter) at 38000 rpm (average centrifugal force 178 305 × g; $\omega^2 t = 1.708 \times 10^{11}$ rad^2/s)/4°C for 3h. After the centrifugation, the liquid was removed by pipetting until reaching the interphase. Then 2 ml of 1 × SALT + 0.5 mM TCEP was carefully pipitted against the walls of the SW41 centrifuge tube to wash the material left on the inner walls of the tube and on the top of the cushion. The washing solution and the sucrose cushion were removed completely by pipetting, and transport RNA granule/polysomal pellet ("Pellet 1") at the bottom of the tube was resuspended in 50 µl of ice-cold 1 × SALT + 0.5 mM TCEP + 0.1% trehalose.

3.1.5 DNase Treatment of "Pellet 1"

To degrade traces of genomic DNA remaining in the Pellet 1, 1 µl of DNase I (ThermoScientific; REF: EN0521; f.c. 1 mU/µl) was added to the "Pellet 1" to the f.c. of 0.01 U/µl, and the sample was incubated on ice for 20 min. In case of a significant material content upon the Dnase treatment, prior to the size exclusion chromatography the volume of the sample was brought up to 80 µl with 1 × SALT+– 0.5 mM TCEP + 0.1% trehalose. The amount of material in Pellet 1 was estimated by measuring A260 in the Nano Drop 1000 spectrophotometer. If the A260 was higher than 30 units, 30 µl of 1 × SALT + 0.5 mM TCEP + 0.1% trehalose were added to the Pellet 1 to increase the yield of the product in the subsequent Sephacryl-S500 gel filtration.

3.1.6 Sephacryl-S500 Gel Filtration

To remove the molecules of the lower weight (e.g. disomes), the DNase I-treated Pellet 1 was centrifuged through 1 ml Sephacryl S500 (GE Healthcare; nominal separation range for dextrans 40 kDa – 20 MDa) size-exclusion spin column. The spin column was prepared by

pipetting 1 ml of sephacryl S500 resin (in 20% EtOH) into an empty Zeba polypropylene column (Thermo Scientific REF. 89882) and centrifugating it at 1000 g/4°C for 1 min to remove the ethanol-containing storage solution. The column was then equilibrated by adding 180 µl of 1 × SALT + 0.5 mM TCEP + 0.1 % trehalose to the centre of the column and centrifugating it at 1000g/4°C for 1 min. The equilibration step was repeated 2 more times. DNase I-treated Pellet 1 was pipetted to the centre of the spin column immediately after the equilibration and centrifuged through it at 1000g/4°C for 1 min. The transport RNA granule containing flow-through (Pellet 1-S500) was aliquoted into precooled Protein LoBind tubes, frozen in liquid nitrogen and stored at -80°C.

3.1.7 Glycogen Removal from Pellet 1-S500 by MBP Coated Ni-Sepharose

20 µl of Ni-Sepharose High Performance (GE Healtcare; dynamic binding capacity of 40 mg His_6-tagged protein per 1 mL resin) resin in 20% EtOH waw washed three times by the addition of ice-cold 500 µl of 1 × SALT + 0.5 mM TCEP, centrifugation in SIGMA 1-14K centrifuge at 100 g/4°C for 15 s and removal of the supernatant. The washed resin was resuspended in 20 µl of 1 × SALT + 0.5 mM TCEP, and 30 µl of a C-terminally His_6-tagged E.coli maltose-binding protein (MPB; cloned and purified by our group; total of 810 µg) was added to the f.c. of 16.2 mg/ml. The mixture was incubated at RT for 15 min on STUART ROLLER MIXER SRT9 with subsequent centrifugation at 100 g/4°C for 15 s to pellet the MBP-bound Ni-Sepharose resin. The supernatant was removed, and unbound MBP was washed away by three repeated washing steps that include the addition of ice-cold 500 µl of 1 × SALT + 0.5 mM TCEP, centrifugation at 100 g/4°C for 15 s and removal of the supernatant. 50 µl of Pellet 1-S500 diluted with 1 × SALT + 0.5 mM TCEP + 0.1% trehalose to the A_{260}=1.0-1.5 was added to MBP-Ni-Sepharose. The mixture was incubated at RT for 15 min on the STUART ROLLER MIXER SRT9, and the resin was pelleted by centrifugation at 100 g/4°C for 15 s. The supernatant is collected to the precooled protein LoBind tube, frozen in liquid nitrogen and stored at -80°C.

3.1.8 Glycogen Removal from Pellet 1-S500 by α-Amylase Digestion

Another tested way to decrease the glycogen contamination was α-amylase (SIGMA A6380) treatment. To assure the successful experiment, the commercial α-amylase was checked for any RNase activity, showing the absence of such. α-amylase was dissolved in 1 × SALT + 0.5 mM TCEP to the f.c. of 33 µg/ml to create the stock solution. Subsequently, 3.6 µl of α-amylase stock was added to 6.4 µl of Pellet 1-S500 with A_{260}=9 diluted with 1 × SALT +

0.5 mM TCEP (f.c. of α-amylase is 11.9 μg/ml). The mixture is incubated at the RT for 30 min. To remove α-amylase the sample was centrifuged in a fixed-angle rotor in a SIGMA 1-14K benchtop centrifuge at 16600 g/4°C for 30 min. During this process, heavy transport RNA granules pellet down but α-amylase remains in solution. The supernatant was removed, and the pellet was redissolved in 6 μl of 1 × SALT + 0.5 mM TCEP.

3.1.9 Glycogen Removal from Pellet 1-S500 by FLX Recombinant Protein

Decrease in glycogen content of the final transport RNA granules preparation was also tested by FLX protein binding. 80 μL of anti-FLAG-M2 resin (Sigma; REF: A2220) was pelleted by centrifugation at 461 g/4°C for 30 s in a SIGMA 1-14K centrifuge. The resin was then washed three times by the addition of the ice-cold 500 μl of SALT500 (HEPES (pH7.5; f.c. 20 mM), KOAc (f.c. 500 mM), MgOAc (f.c. 4 mM), TCEP(f.c. 0.5 mM)), centrifugation at 461/4°C for 30 s and supernatant removal. The resin was mixed with 50 μl of 10 μM FLX (cloned and purified by our group) and incubated for 10 min at RT with the constant rolling between the fingers in an upright position to achive the equal distribution of the resin in the buffer. The resin was pelleted by the centrifugation at 461 g/4°C for 30 s and washed three times by the addition of the ice-cold 500 μl of SALT150 (HEPES (pH 7.5; f.c. 20 mM), KOAc (f.c. 150 mM), MgOAc (f.c. 4 mM), TCEP (f.c. 0.5 mM)) and repeated centrifugation followed by the supernatant removal as described above. The resin with bound FLX was resuspended in 50 μl of Pellet 1-S500 (diluted with SALT150 to A_{260}=4) and incubated at RT for 10 min with constant rolling between the fingers. The resin was pelleted by centrifugation and washed three times with 500 μl of ice-cold 1 × SALT + 0.5 mM TCEP followed by the steps of centrifugation and supernatant removal as described above. The bound transport RNA granules and polysomal material was eluted by resuspending the resin in 50 μL 1 × SALT + 0.5 mM TCEP containing 150 μg/mL 3 × FLAG Peptide and incubated at RT for 10 min with constant rolling between fingers. The resin was pelleted down by centrifugation at 461 g/4°C for 30 s, and the supernatant is transferred to a separate protein LoBind tube. Such elution was performed 4 times to increase the yield, and the first three eluates were pooled. The resulting pooled eluate was centrifuged at 16000 g/4°C for 30 min to pellet down the transport RNA granules. Upon removal of the supernatant, resulting pellet is dissolved in 6 μl of 1 × SALT + 0.5 mM TCEP.

3.1.10 Negative Staining of Transport RNA Granules Preparations

Quantifoil grids (100 Holey Carbon Film, Cu 200 mesh; agar scientific) coated with a 3 nm carbon layer were glow-discharged at 0.45 mBar and 10 mA for 15 s in a Pelco easiGlow glow discharge system (TED PELLA, INC.). 4 µl of the sample were immediately pipetted to the carbon-coated face of the grid, and the grid was incubated at RT in a humidity chamber for 3 min. The grids were washed three times in the 1 × SALT + 0.5 mM TCEP solution and dried by wicking the grid with the filter paper. The sample was twice stained by 4 µl of 2% $U(OAc)_2$ for 1 min with the removal of the dye with the filter paper. The grid was additionally dried for 6 min under a halogen lamp at RT and stored in the desiccator chamber until visualisation.

3.1.11 Polysomal Profiling to Investigate the Effect of Homoharringtonine Treatment

Before harvesting, three cell culture dishes were treated with CHX (f.c. 100 µg/ml), HHT (Cayman Chemical Company; REF: 14631; f.c. 10 µM) or DMSO (f.c. 0.027% by volume) for 40 min. The dishes were suqsequently washed two times with 5 ml ice-cold isotonic HBSS-EGTA solution. The cells were harvested by the cell scraper in 2 ml of ice-cold HBSS-EGTA solution containing the respective antibiotic or DMSO. Cell suspensions were pelleted by centrifugation in a fixed-angle rotor in a SIGMA 1-14K benchtop centrifuge at 200 × g/4 C for 5 min, the supernatant was removed, and the cell pellet was resuspended in 250 µl of RBS solution (10 mM Tris-HCl (pH 7.5), 10 mM KOAc, 2.5 mM $Mg(OAc)_2$ 1 mM TCEP , Ribolock (f.c. 0.107 U/ml), ROCHE protease inhibitor tablet (1 tablet/3 ml)) with the respective compound (CHX (f.c. 0.2 mg/ml); HHT (f.c. 20 µM); DMSO (f.c. 0.05%)). The cell suspensions were mixed with 250 µl of the extraction buffer (1 × RBS, Triton-X100 (f.c. 2%), Tween-20 (f.c. 1%), Na-deoxycholate (f.c. 1%)) followed by the incubation on ice for 5 min. The cell debris were pelleted by centrifugation in a fixed-angle rotor at 16600 × g/4 C for 5 min, and the supernatants were pipetted on the top of 10%-50% sucrose gradient in in 1 × SALT + 0.5 mM TCEP. The gradients were prepared as follows: 5.5 ml of 10% sucrose solution is pipetted to the SW41 tube, and 5 mL “LuerLock” syringe fitted with HAMILTON NDL N 6 needle was inserted in the solution, 5.5 ml of 50% sucrose was pipetted in the syringe and slowly released in the 10% sucrose solution letting the denser 50% sucrise sink to the bottom. The polysomal, 80S and subunit fractions were resolved in the gradients by centrifugation at 140703 g /4°C for 105 min in Optima XE-90 ultracentrifuge in a Ti SW41 rotor. The gradients were analysed by BioRad ECONO UV

Monitor during the process of their pumping trough the device with SPETEC PERIMAX 12/1 SM peristaltic pump (pumping rate – 90 rpm). The A_{260} was recorded with the sensitivity of 0.2 AUFS using the WindDaq programme. 1 × SALT + 0.5 mM TCEP was used for blanking and washing upon moving to the next gradient.

3.1.12 Western Blot

To compare the content of the preparations from Pellet 1-S500, FLAG purified Pellet 1-S500 and rat cortical material were analysed by western blot. The preparations were diluted to 40 µl with double distilled H_2O (ddH_2O), and the dilutions were divided into two aliquots. Each of two replicate aliquots contained: 0.02 A_{260} U of Pellet 1-S500, 0.003 A_{260} U of FLAG purified Pellet 1-S500 and 0.019 A_{260} U of rat cortical RNAg. The samples were mixed with 4 µl of home-made SDS Loading Dye and incubated at 95°C for 5 min to denature the proteins. The samples were loaded on the 10% SDS-PAGE gel, and electrophoresis was performed at 180 V/RT for 1 h. Subsequently, the proteins were transferred from the polyacrylamide gel to the 0.45µm pore size Immobilon-P membrane (Merck; IPVH08130) in the BioRad wet transfer units as follows: the polyacrylamide was rinsed in 10 ml pf PVDF buffer (Tris-base (3.05g/l), glycine (14.4 g/l), MeOH (SIGMA; REF: 34885-1L-M; 25 ml/l of the final volume)) and laid on a stack of 3 filter papers of the matching size (prewetted in PVDF), the membrane cut to the same size and prewetted in MeOH was put on the top of the gel and covered with extra 3 layers of filter papers prewetted in PVDF. Filter papers, gel and membrane assembly was fixated in the transfer rack, and the proteins were transferred ain the PVDF buffer at 80 V/0.18 A/ 14 W/4°C for 85 min. Upon the completion of the transfer, which was visible due to the presence of the ladder bands on the membrane, the membrane was rinsed in 10 ml of TBST buffer (Tris-HCl (pH 7.5; f.c. 0.05 M), NaCl (f.c. 0.15 M), Tween-20 (0.05% by volume)) to wash away the residual MetOH. Then the membrane was transferred to the 10 ml 5% milk-TBST solution (nonfat dried milk powder BC (AppliChem; A0830,0500) used) in a square Petri dish (Electron Microscopy Sciences; REF. 70691) for blocking. The blocking was performed at RT for 1 h in an orbital-shaker. The membrane was cut into two halves and they were soaked in two different solutions of primary antibodies in 10 ml of 5% milk-TBST. Solution 1 contained anti-rpL7a/SURF3 (Bethyl Laboratories Inc. REF: A300-749A-T; 4 µl/10 ml), anti-Caprin-1 (Invitrogen; REF: PA5-96857; 7 µl/10 ml), anti-G3BP-1 (Millipore; REF: 07-1801; 6 µl/10 ml). Whereseas, solution 2 had anti-rpL7a/SURF3 (Bethyl Laboratories Inc. REF: A300-749A-T; 4 µl/10 ml) and anti-G3BP-2 (Invitrogen; REF: PA5-53776; 6 µl/10 ml). The membranes were

incubated in respective primary antibody solution at RT for 50 min in an orbital-shaker. Binding of the primary antibodies is followed by three washes of the membranes in 3 × 10 ml of TBST (2 min per wash). Washed membranes are transferred to the 10 ml 5% milk-TBST solution containing secondary antibody (peroxidase-conjugated goat anti-rabbit IgG (H +L) HRP (Pierce; 31466; 1 µL/10 mL)) and incubated for 50 min in an orbital-shaker. The incubation with the secondary antibody is followed by three washing that are identical to described above. The membranes were then soaked in 1 mL ECL developing solution (freshly prepared by mixing reagent 1 and reagent 2 (Amersham ECL Western Blotting Analysis system; RPN2109) in 1:1 volume ratio) within plastic sleeves, the sleeves were placed in a cassette and exposed to a chemiluminescence film (GE Healthcare) at RT for 1 min.

3.1.13 Cell Confluency Quantification

The confluencies of the adherent cell cultures were estimated from phase contrast microscopy images following the strategy described by Busschots *et al.* 2015. For the estimation of confluency, 5 grayscale 8-bit phase-contrast images (size 2560 × 1920 pixels) of cells from each of the Thermo Scientific BioLite 130183 15 cm cell culture dishes were acquired. The images were processed and the confluency calculated using an in-house Matlab script written to enable a quick and unbiased processing of a large number of images (typically 40 images per single timpoint). The pixel intensity scale of the original grayscale images was inverted, followed by background subtraction and binarization of the background-subtracted images using Otsu's thresholding as implemented in the Matlab imbinarize function. The interior pixels form each cell were removed using the inbuilt Matlab bwmorph function, followed by a morphological dilation and erosion of the cell contours using a 20-pixel sized circular structuring element (kernel). The areas under the morphologically processed cells (in square pixels) were calculated using the inbuilt Matlab bwarea function. The confluency for each image was calculated as the ratio of the total area under the cells to the total area of each 2560 × 1920 pixel image. To enable an approximate estimation of the number of cells on the dishes without the need to remove the cells for counting, cells were grown in a separate experiment on four 10 cm culture dishes (Thermo Scientific BioLite 130181) and the confluencies estimated from the phase contrast images as described above. The cells were subsequently detached from the dishes by treatment with trypsin and the number of cells counted using the CytoSmart cell counter as described in the next paragraph. The cell

count was correlated to the estimated confluency, yielding a conversion factor of 830 cells/cm^2 for a 1 % confluency.

3.1.14 Cell Culturing for the Gene Expression Analysis

SH-SY5Y cells were seeded on 6 × 6 cm culture dishes (Thermo Scientific BioLite; REF: 130180; culturable area 20.5 cm^2) and grown at 37°C in the humid atmosphere of 5% CO_2 in 5 ml of "full" DMEM medium. Upon reaching the confluency of 60%, 100% of the serum-containing "full" DMEM medium was removed and replaced with 5 ml "full" Neurobasal medium. 3 of the dishes (half) were supplemented with 15 µM ATRA (ATRA series), and another 3 dishes were mock-treated with 0.066% DMSO (control series). The 0.066 % DMSO in the control series is equal to the DMSO concentration in the medium in the ATRA series. The cells were cultured for 5 days , by which time the cultures reached an approximate confluency of 100%. On day 4 50% of the current medium was replaced with the fresh medium containing the respective compound. Cells were harvested in 1 ml of isotonic HBSS solution using a cell scraper. Cell suspensions were transferred to the precooled 2 ml polypropylene tubes using a large cut pipette tip to avoid the mechanicall damage of the cells. The cells were pelleted by centrifugation at 200 g/4°C for 5 min. The supernatant was discarded, and the pellet was resuspended in 100 µl of ice-cold HBSS. 10 µl aliquots were used for the cell counting, rest of the cell suspension was frozen with liquid nitrogen and stored at -20°C for the total RNA extraction. The aliquots for cell counting were mixed with 100 µl of trypsin-EDTA solution, the suspensions were homogenised by pipetting and incubated at 37°C for 2 min. The incubation was followed by the addition of 500 µl of "full" DMEM to inactivate the trypsin. 10 µl of the trypsinised cells diluted with "full" DMEM medium was mixed with 10 µl of Trypan Blue (f.c. 0.2%) for the staining and pipetted to the wells of a CytoSmart hemocytometer plate. The cell counting was performed on a CytoSmart Cell Counter on 5 different locations on the hemocytometer plate using the following cut-off criteria for cell detection.

3.1.15 Total RNA Extraction

To obtain the substrate for the reverse transcription reaction and RT-qPCR analysis, total RNA from ATRA differentiated and non-differentiated cells (3 × 6 cm dishes each series) had to be extracted. To extract the total RNA 100 µl aliquots of previously obtained cell suspensions were acidified by the addition of 11.3 µl of 3M NaOAc (pH 5.3; f.c. 0.3 M). The samples were mixed with the phenol pH 4-5 (SIGMA; REF.

77619):chlorophorm:isoamyl alcohol (125:24:1) in the volume ratio of 1:1 and the mixtures were vortexed for 15 s with subsequent centrifugation at 16600 g/4°C for 5 min in the SIGMA 1-14K centrifuge. Upon the centrifugation, the aqueous phases were collected. To extract the RNAgs in the remaining aquous phases 100 µl of 3M NaOAc (pH 5.3) was added to the original samples, the mixtures were vortexed for 15 s, and the centrifugation at 16600 g/4°C for 5 min was repeated. The newly appeared aqueous phases were collected and pooled with the previously obtained. Chloroform was added to the collected aqueous phases in the volume ratio of 1:1, the mixtures were vortexed for 15 s, and the phases were separated by centrifugation at 16600 g/4°C for 5 min. The aqueous phases were collected. Remaining transport RNA granules were back-extracted by the addition of 50 µl of 3M NaOAc (pH 5.3) to the chloroform, vortexing for 15 s and centrifugation at 16600 g/4°C for 5 min. The new aqueous phases were added to the previously collected. To remove the residual chlorophorm and phenol 96% EtOH (Chem-Lab; CL00.0556.0250) was added to the collected aqueous phases in the volume ratio of 2.5:1. The mixtures were vortexed for 15 s and incubated at -20°C for 1 h. The precipitated samples were centrifuged at 16660 g/4°C for 15 min, and the supernatants were discarded. The pellets were washed adding 900 µl of ice-cold 70% EtOH and centrifugating at 16600 g/4°C for 15 min. The supernatants were removed, and the samples were dried for 5 min at RT to let the residual ethanol evaporate. RNA preparations were resuspended in 40 µl of ultrapure H_2O (Invitrogen; REF. 10977-035). To degrade genomic DNA in the sample 5.6 µl of 10 × RQ1 buffer (TRIS-HCl pH 7.5; f.c. 400mM), $MgSO_4$ (f.c. 100 mM), $CaCl_2$ (f.c. 10 mM), RNase-free H2O) and 10 µl of RQ1 RNase-free DNase (Promega; REF. M6101; f.c. 0.18 u/µl) were added to the redissolved RNA preparations, and the mixtures were incubated for 30 min at 37°C. Upon the completion of the DNase treatment, the volumes of the samples were brought up to 100 µl with the ultrapure H_2O. Silica spin-columns of QIAGEN Rneasy Mini Kit were used for further purification of the sample according to manufacturer's instructions. The RNA was eluted from the columns by pipetting 30 µl of ultrapure H_2O to the centre of the column and centrifuging it at 12470 g/4°C for 1 min. The elution step was repeated using the previously obtained elute instead of ultrapure H_2O to maximise the yield of the product. RNA preparations were stored at -20°C.

3.1.16 Reverse Transcription

Reverse transcription premix (2.2 reactions) was prepared by adding 28.8 µl of H2O to 4.4 µl of 10 × RT Reaction Premix with Oligo (dT) + random Primers (Solis BioDyne; REF. 06-

20-00100). 15.1 μl of the premix was pipetted in the PCR tube, and 3.4 μl of diluted to 100 ng/μl sample was added. The mixture was incubated at 70°C for 5 min with the subsequent incubation on ice for 2 min and addition of 1.5 μl of FIREScript Enzyme mix. The programme for the PCR machine was set as follows: 25°C for 7 min – 40°C for 15 min - 85°C for 5 min.

3.1.17 RT-qPCR

The PCR reaction mix contained 2 μl of 5 × HOT FIREPol EvaGreen qPCR Mix Plus (SolisBioDyne), 1 μl of the DNA template, 1 μl of each primer (f.c. 0.25 μM) and 5 μl of H_2O (total volume 10 μl). The reaction was carried out in duplicate in the 384 well plate (BIOplastics BV; REF: B70515L) sealed with Opti-Seal Optical Disposable Adhesive (BIOplastics BV; REF: 157300). Before the initiation of the reaction, the plate was spinned down for 1 min at 1800 rpm and 20°C in an Eppendorf Centrifuge 5810R using A-4-62 swing-out rotor. The RT-qPCR programme was set in Applied Biosystems 7900HY Fast Real-Tome PCR System (Applied Biosystems) as follows: 95°C for 12 min, [95°C for 15 s, 60°C for 20 s, 72°C for 20 s] × 40, 95°C for 15 s, 60°C for 15 s.

3.1.18 Primer Design

The primers used are FW_dlg4 (forward primer for DLG4 gene; sequence: AG-TGGTCAAGGTTAAAGGCCAAG), RV_dlg4 (reverse primer for DLG4 gene; sequence: TTCCATCTGCGTCACTGTCTC), FW_ache (forward primer for ACHE gene; sequence: TGGAGACTTCCTCAGTGACACC), RV_ache (reverse primer for ACHE gene; sequence: ATACGAGCCCTCATCCTTCACC), FW_ncam2 (forward primer for NCAM2 gene; sequence: CAGCAGAGAGAGGAGAAGAAATGAC), RV_ncam2 (reverse primer for NCAM2 gene; sequence: CAATGAGCTTGCCATTCCTGAAC), FW_syn1 (forward primer for SYN1 gene; sequence: CCCCAGTGTTAACTCCTTGCATTC), RV_syn1 (reverse primer for SYN1 gene; sequence: TGTCCCCAGTTTCTTATGCAGTC), FW_ntng2 (forward primer for NTNG2 gene; sequence: GTTCTGCTCCCATGA-GAATCCC), RV_ntng2 (reverse primer for NTNG2 gene; sequence: TCCTT-GTCGAACATGAGCCTG), FW_kcnma1 (forward primer for KCNMA1 gene; sequence: TGAGTAGCAATATCCACGCGAAC), RV_kcnma1 (reverse primer for KCNMA1 gene; sequence: AGGAAGAGGAGGAGGAAGAAGAAG), FW_gapdh (forward primer for GAPDH gene; sequence: TCAAGATCATCAGCAATGCCTCC), RV_gapdh (reverse primer for GAPDH gene; sequence: GTCATGAGTCCTTCCACGATACC), FW_cdk1

(forward primer for CDK1 gene; sequence: GCTTTGGGCACTCCCAATAATG), RV_cdk1 (reverse primer for CDK1 gene; sequence: GGATGCTAGGCTTCCTGGTTTC). The primers were designed using EuroFins Genomics qPCR Primer and Probe Design Tool with the following criteria: location in the gene coding sequence, length of 18-30 nt, GC content 40-55%, T_m 54-56°C, amplicon length 70-100 bp. The nucleotide sequences of the target-mRNAs were retrieved from the NCBI Nucleotide Database. The presence of the primer binding sites on all splicing variants (mRNA isoforms) of a given mRNA transcript was verified by multiple sequence alignment using VectorNTI software (Invitrogen).

3.1.19 RT-qPCR Statistical Analysis

Statistical analysis was performed by assuming that the errors follow normal distribution and calculating standard deviation based on C_t values Theoretical standard deviation was adjusted using Cochran's theorem, and the real standard deviation was calculated with 95% confidence. The upper value of the standard deviation was used to evaluate the statistical significance of the data by the empirical rule using two standard deviations as a critical value. Only genes with both replicates being statistically significant are considered to be such themselves. As the expression of GAPDH is known to remain constant upon ATRA treatment of SHSY-5Y, sample C_t values in the ATRA treated and nontreated sample were normalised to the C_t value of the GAPDH gene (Castano and Kypta, 2008).

3.2 RESULTS

3.2.1 Cellular Glycogen is a Major Contaminant in the RNA Granule Preparation from SH-SY5Y

High purity and homogenous preparation of transport RNA granule macromolecules is required for the single-particle cryoelectron microscopy and proteomics analyses, resulting in a need for a complex and multistep purification procedure. Initial purification of the crude preparation of ribosomes and ribosomal complexes is often performed using velocity sedimentation through a dense sucrose cushion. Separation by velocity sedimentation is based on the exclusively high molecular mass of the ribosome (over 1 MDa) compared to the majority of the cellular macromolecules. Thus, the ultracentrifugation is performed through the 60% sucrose cushion under appropriate ionic conditions. After ultracentrifugation, heavy transport RNA granules and polyribosomes sediment while lighter macromolecules (80S monosomes and lighter polysomes) remain in the supernatant. The pellet is then redissolved in the appropriate buffer and treated with DNase to remove the contaminating genomic DNA and the associated DNA-protein complexes. Depending on the number of cells harvested, the yield of the ribosomal material in "Pellet 1" ranges from 4 to 44 picomoles 80S equivalents (0.08 to 0.47 pmol/106 cells). DNase-treated material is further purified by size exclusion chromatography in a Sephacryl S500 spin column. Size exclusion chromatography is based on the temporary trapping of particles with a lower size in the pores of the resin, while larger particles are constrained to move in the interstitial liquid and therefore elute faster in the void volume. According to the results of our group obtained with rat cortical material, Sephacryl S500 spin columns are efficient in enriching the crude preparations for transport RNA granules over polyribosomes. Depending on the amount of the starting cell mass, the yield of the material in the Sephacryl S500 purified RNA granule preparation (called "Pellet 1 – S500") ranges from 0.4 to 22.4 picomoles (0.04 to 0.24 pmol/106 cells). However, when the Sephacryl S500 purified RNA granule preparation was analysed by negative stain electron microscopy, we mostly observed lighter-stained spherically shaped particles with a ca. 100 nm diameter with occasionally occurring darker-stained particles similar to the RNA granules from rat cortex (Fig.1). Differently from the RNA granules, these dominant lighter-staining particles are resistant to an RNase, protease and high-salt treatment and are identical to cellular glycogen granules visualised by negative stain electron microscopy (Sullivan *et al.,* 2010). The presence of glycogen in the RNA granule preparation is in agreement with the results of our earlier colourimetric

analysis of the RNA granule preparation using the hexose-specific anthrone-sulfuric acid test (Hörmann and Gollwitzer, 1962). Thus, while the combination of velocity sedimentation and Sephacryl S500 size exclusion chromatography can separate the heavy-sedimenting and larger-sized RNA granules from smaller ribosomal complexes, it fails to separate RNA granules from the similarly sized glycogen granules. Therefore, we have faced the demand to investigate the techniques to remove the glycogen.

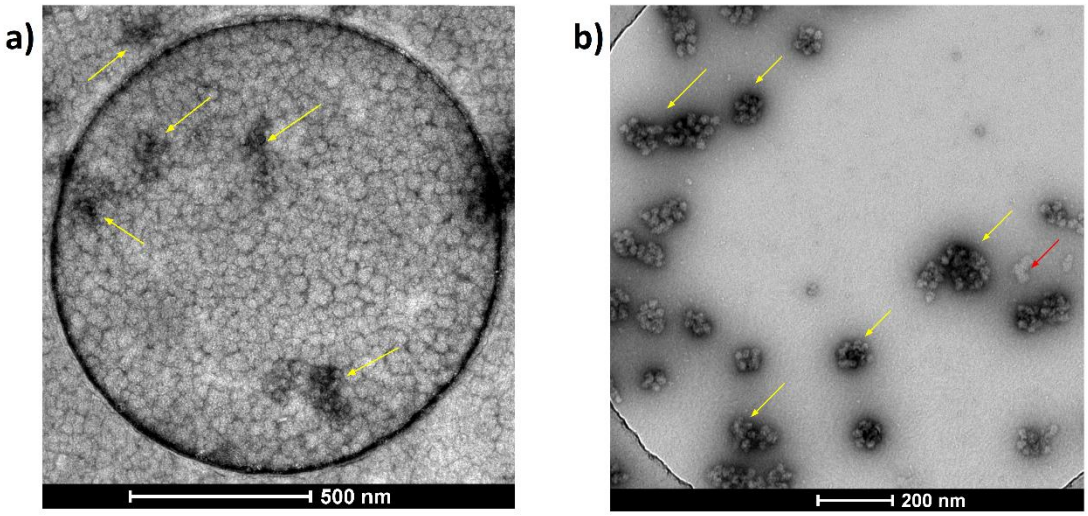

Figure 1: Electron microscopy pictures of negatively stained transport RNA granule preparations; yellow arrows mark transport RNA granules, red – glycogen. a) transport RNA granule sample purified from neuroblastoma; b) transport RNA granule sample purified from rat cortical material

3.2.2 Insulin Deprivation During Cell Culturing Does not Effect the Glycogen Deposition

Cellular glycogen storage is regulated by the hormone insulin. Insulin upregulates glycogen storage by facilitating glucose uptake via an increase in the glucose specific transporters and activity of glycogen synthase, inactivating glycogen synthase kinase (Muhič *et al.*, 2015). Searching for a means to reduce the glycogen contamination during cultivation, we, therefore, tested the differentiation of SH-SY5Y in an insulin-free Neurobasal growth medium. Based on the confluency of cell cultures, the absence of insulin significantly decreased cellular proliferation rate over the entire differentiation period (Fig.2). However, despite the markedly decreased proliferation rate of the cells in the absence of insulin, qualitatively similar glycogen contamination was observed in the RNA granule preparations extracted from the insulin-free and insulin-containing cultures (Fig.3).

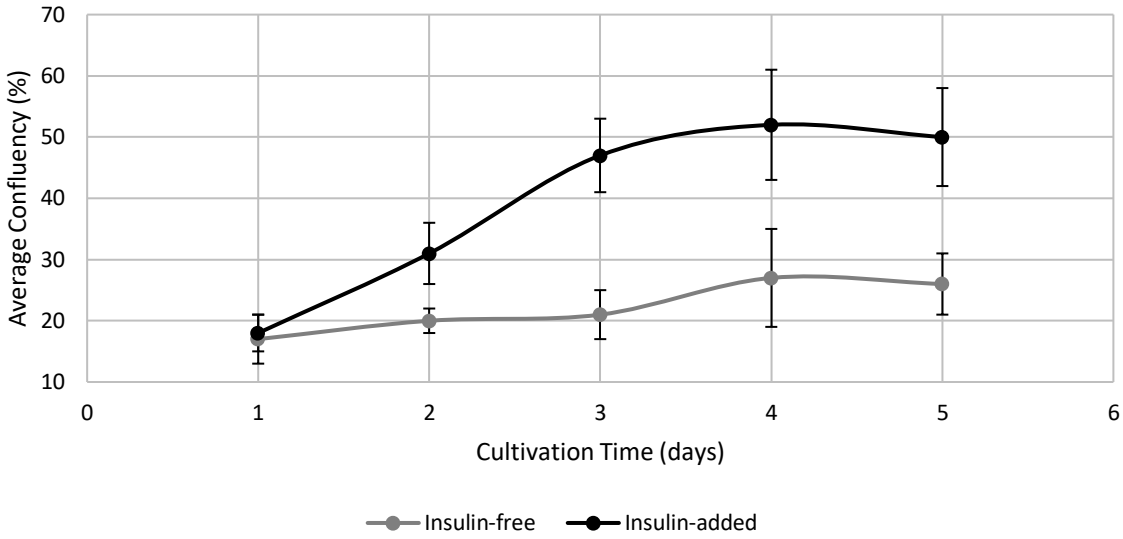

Figure 2: Average confluency onfluency calculated during 4 days of culturing is plotted for cells grown in the medium containing insulin (insulin-added) and insulin-free medium (insulin-free).

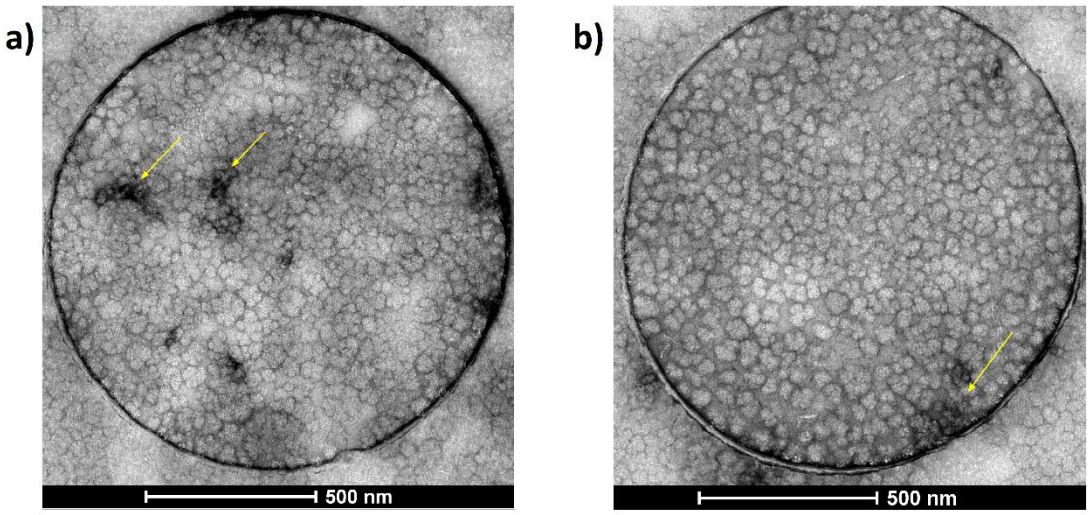

Figure 3: Electron microscopy pictures of negatively stained transport RNA granule preparations; yellow arrows mark transport RNA granules; a) transport RNA granule preparation from neuroblastoma cells cultured in the insulin-containing medium; b) preparation from neuroblastome cells cultured in the insulin-free medium

3.2.3 α-Amylase Treatment Does not Effectively Decrease the Glycogen Contamination

α-Amylase, a glycosyl hydrolase that catalyses the hydrolysis of α(1→4) glycosidic linkages in starch, is also known to efficiently digest glycogen and for this reason has been used to degrade the glycogen particles in tissue preparations for electron microscopy analysis

(Coimbra 1966). We, therefore, first attempted to remove the contaminating glycogen from the Sephacryl S500 purified transport RNA granule preparation by α-amylase digestion. Nevertheless, the decrease in the glycogen content upon such treatment is neglectable (Fig.4).

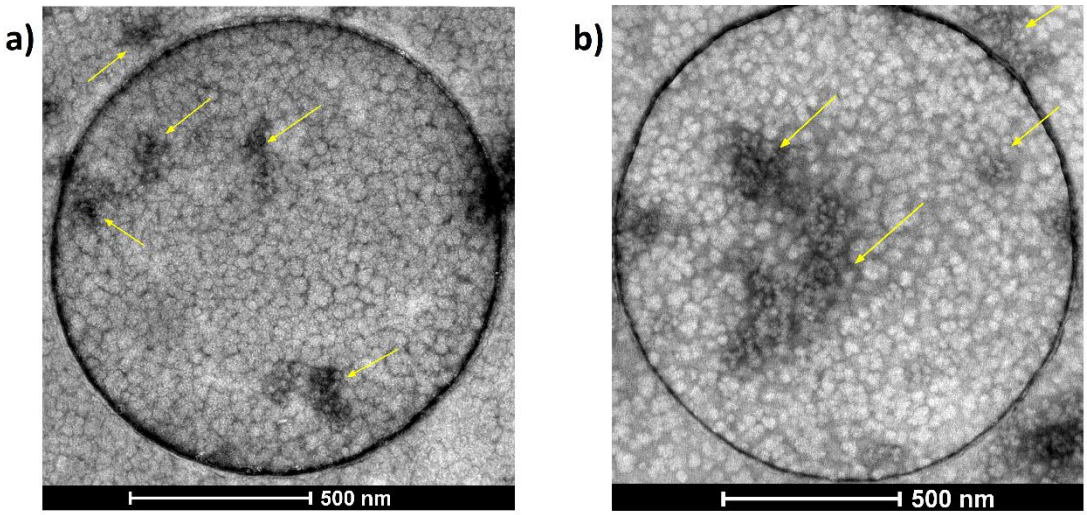

Figure 4: Electron microscopy pictures of negatively stained transport RNA granule preparations; yellow arrows mark transport RNA granules; a) transport RNA granule sample purified from neuroblastoma, without glycogen removal; b) amylase-treated transport RNA granule sample purified from neuroblastoma

3.2.4 Maltose Binding Protein Immobilised on Ni-Sepharose is Capable of Glycogen Removal

Since the α-amylase digestion failed to remove glycogen from the transport RNA granules preparation, we tested whether glycogen contamination can be decreased by affinity chromatography on a Ni-Sepharose resin. As Ni-Sepharose resin is specific for proteins containing a hexahistidine tag that is absent in glycogen, we used different proteins as adaptors. In the first experiment, we sought to use Ni-Sepharose affinity resin to remove the glycogen granules from the Sephacryl purified transport RNA granule preparation. Ni-Sepharose efficiently binds histidine-tagged proteins. To remove glycogen, we used a C-terminally His6-tagged *E.coli* Maltose Binding Protein (MBP) as an adaptor molecule bound to the Ni-Sepharose resin. Though natural substrates of MBP are maltose and maltodextrins, it is known to bind a number of polysaccharides (including glycogen) containing α(1→4) linked glucose monomers (Walker *et al.*, 2010). Hence, the contaminating glycogen granules can be bound to the MBP-coated Ni-Sepharose resin while the RNA granules

remain in the liquid phase and can be separated from the resin in the supernatant by low-speed centrifugation. In line with our expectations, a majority of the glycogen particles were removed from 10 µl of Sephacryl S500 purified transport RNA granules preparation after 10 min incubation on 20 µl of MBP-Ni-Sepharose resin (Fig.5a). The darker-staining particles in the supernatant appear outwardly similar to rat cortical RNA granules (Fig.1b). In a separate experiment instead of 10 µl, we have purified 40 µl of a Sephacryl S500 purified transport RNA granule preparation with 20 µl of MBP-Ni-Sepharose resin, and a noticeable amount of glycogen was observed in the supernatant by electron microscopy (Fig.5b). This observation indicates that the ability of the MBP-Ni-Sepharose to remove glycogen is limited by the binding capacity of the resin. Therefore, for a successful purification, the volume of transport RNA granule sample relative to the volume of the MBP-coated resin needs to be kept below 1:2 volume ratio.

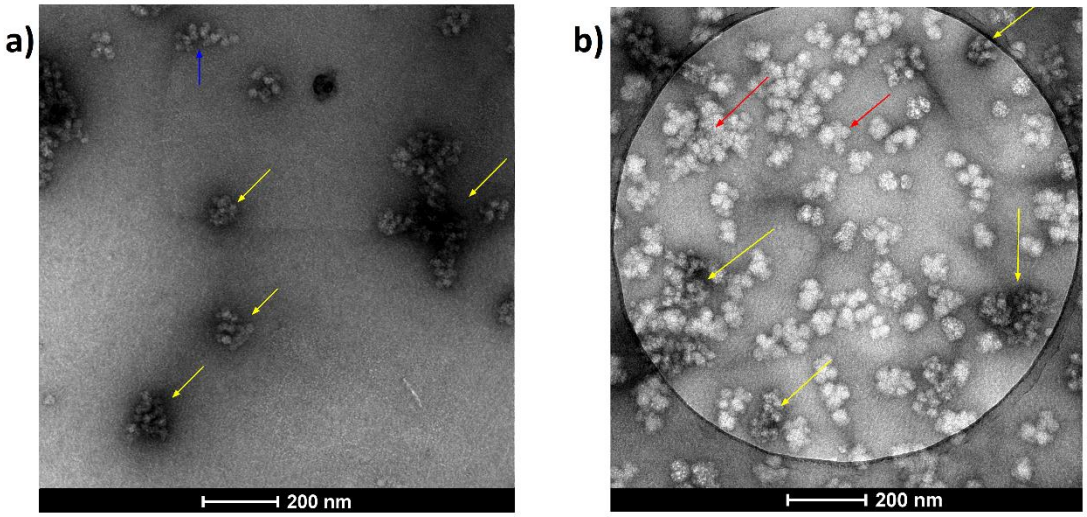

Figure 5: Electron microscopy pictures of negatively stained transport RNA granule preparations; yellow arrows mark transport RNA granules, red – glycogen, blue – polysomes. a) transport RNA granule preparation from neuroblastoma purified with MBP affinity chromatography (voulme ratio sample:MBP-Ni-Sepharose – 1:2); b) transport RNA granule preparation from neuroblastoma purified with MBP affinity chromatography (voulme ratio sample:MBP-Ni-Sepharose – 2:1)

3.2.5 FLAG-tag Affinity Chromatography Efficiently Purifies RNA Granules from Contaminating Glycogen

Though the preceding experiment shows that glycogen can be efficiently removed from the transport RNA granule preparation on the MBP-Ni-Sepharose resin, a binding of poly(A)

containing mRNAs to the Ni-resin has been reported (Nastasijevic *et al.*, 2008). Additionally, unpublished results of our group indicate that key RNA granule components like CAPRIN-1 bind to the Ni-resin. Hence, the mRNA-containing RNA granules, as well as their protein components, may be partially lost during the purification on the MBP-Ni-resin. We, therefore, tested a different affinity purification of the RNA granule preparation using FLAG-resin. FLAG is a short peptide sequence (AspTyrLysAspAspAspAspLys) which serves as an epitope, allowing for the affinity chromatography of the proteins it is fused with (Hopp *et al.*, 1988). Anti FLAG M2 is a monoclonal antibody which is expressed in mouse and allows for the recognition and binding of the FLAG epitope (Sigma-Aldrich). For affinity purification, anti FLAG M2 is covalently immobilised on the resin to enable easy extraction of the FLAG-tagged proteins. As the transport RNA granules do not contain FLAG epitope themselves, as an adaptor molecule we have used a protein that we called FLX with an ability to simultaneously bind to the FLAG resin and RNA. FLX is an artificial protein that has the FLAG-tag sequence at its N-terminus, *E. coli* ribosomal protein L9 flexible helix as a linker and positively charged (high content of Arg, Lys, His) protein at its C-terminus. Thus the transport RNA granules in the Sephacryl S500 purified preparation bind to the Flag-resin while the unbound glycogen particles are removed during the washing step. The bound RNA granules are subsequently eluted from the resin using a peptide with a sequence identical to the FLAG epitope. Most of the RNA-containing material was eluted during the second elution with a significant amount of material being present in the first and third fraction as well (Fig. 6). Thus, the first three fractions were combined. As shown by an electron microscopy analysis of the combined FLAG-eluted fractions, most of the glycogen present in the initial Sephacryl S500 fraction is removed following the FLAG-tag affinity purification (Fig.7). However, as FLX bound to the RNA non-specifically, polysomes are found in the sample as well.

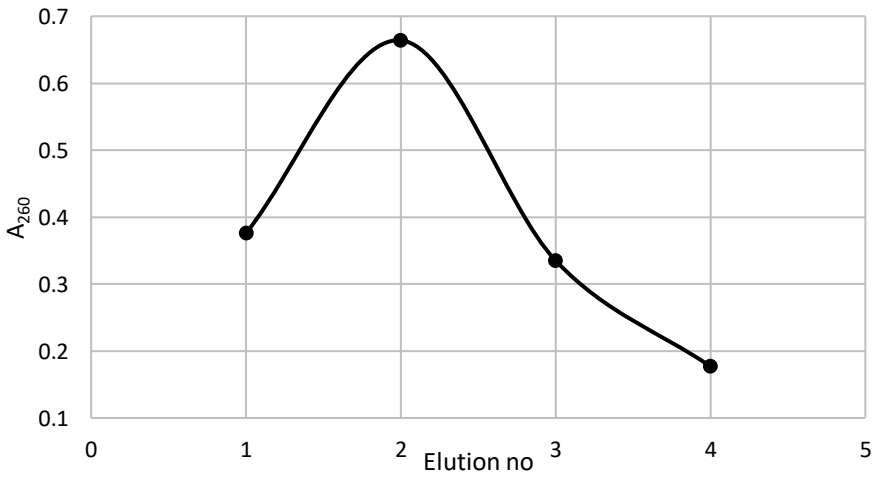

Figure 6: The A_{260} of eluted from FLAG-tag resin transport RNA granule preparation is plotted against the number of elution step.

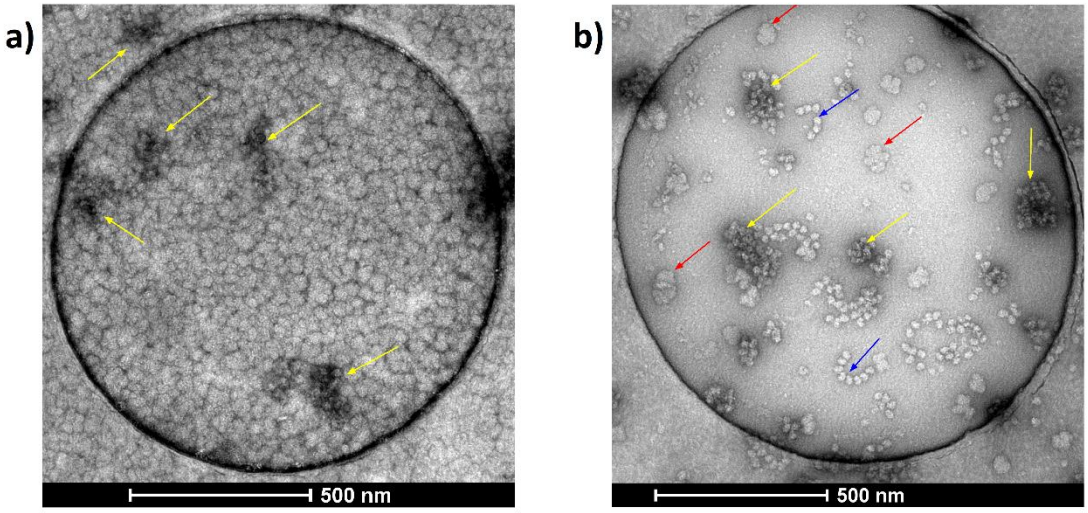

Figure 7: Electron microscopy pictures of negatively stained transport RNA granule preparations; yellow arrows mark transport RNA granules, red – glycogen, blue – polysomes. a) transport RNA granule sample extracted from neuroblastoma, without glycogen removal; b) transport RNA granule sample extracted from neuroblastoma, purified with FLAG-tag affinity chromatography.

3.2.6 The Culture Needs to Reach High Confluency for the Significant Yield of Transport RNA Granules

Adherent cells are usually cultivated to less than 100 % confluency to avoid introducing stress and changes in cell physiology and gene expression. Therefore, we initially harvested the cells for the transport RNA granule extraction upon reaching the average confluency of 60-90% % (average of 10 × 107 for the total number of cells on 8 × 15 cm culture dishes) However, the amount of material obtained after the multistep purification was insufficient for the downstream purification and analysis. A larger amount of the starting cell mass is therefore required for obtaining RNA granules in sufficient quantities. The amount of the cell mass can in principle be increased by growing the cells on a larger number of dishes. Nevertheless, an increased number of the culture dishes leads to the practical problems of handling of the cells during harvesting as all the manipulations with the cells have to be performed within a short time to avoid perturbing cell physiology before cell lysis. Besides, each additional culture dish increases the costs of the experiments. Thus, to increase the starting cell mass we decided to let the cells differentiate in ATRA supplied “full” neurobasal medium for 5 days to confluency above 100%. During this period, the average number of cells on 8 × 15 cm culture dishes reaches 13 × 107. With such an amount of initial cell mass,

sufficient quantities of the transport RNA granules could be obtained. Assuming, most of the RNA (absorbance at 260 nm wavelength) in the preparation comes from ribosomes, we have approximated the concentration of 80S by conversion of A260. Considering the average number of the 80S in one transport RNA granule to be 12-13, the concentration of transport RNA granules was calculated (Fatimy *et al.*, 2016) (Fig.8).

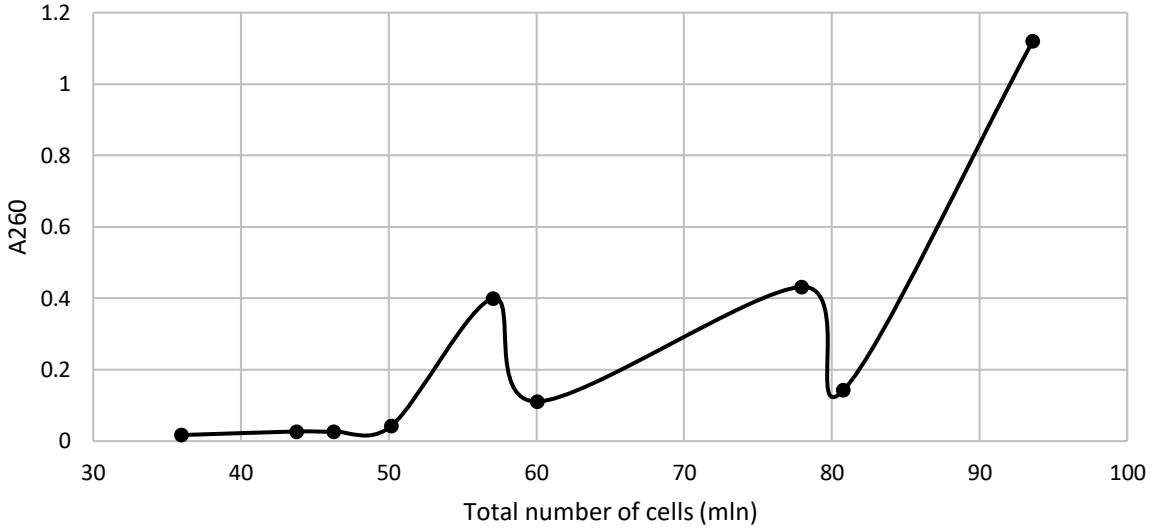

Figure 8: The amount of extracted RNA granules in A_{260} units plotted against the total number of cells harvested for RNA granule extraction. The number of cells was estimated based on the cell confluency in the phase-contrast images using the 830 cells/cm 2 = 1 % confluency conversion factor (described in paragraph 3.1.13 in the Methods section) and the 148 cm 2 culturable area for one 15 cm diameter cell culture dish.

3.2.7 RA Treatment Changes Morphology of the Neuroblastoma Cells to be more Neuron-Like and Alters the Gene Expression Pattern

The differentiation of SH-SY5Y using ATRA is based on previously established protocols (Shipley *et al*., 2016). In line with previous observations, a neuronal-like morphology with numerous extended neurites and more pyramidally shaped cell bodies become apparent following a 5-day ATRA treatment (Fig.9). Besides in agreement with previous studies, the proliferation rate of SH-SY5Y was decreased by 73% after a 5-day ATRA treatment compared to DMSO mock-treated SH-SY5Y. To confirm the differentiating effect of ATRA under chosen culturing conditions in more detail, we analysed changes in the expression levels of several transcripts related to neuronal function using RT-qPCR. The chosen mRNAs have been previously shown to change their expression level upon RA treatment in SH-SY5Y (Korecka *et al*., 2013; Forster *et al.*, 2016).

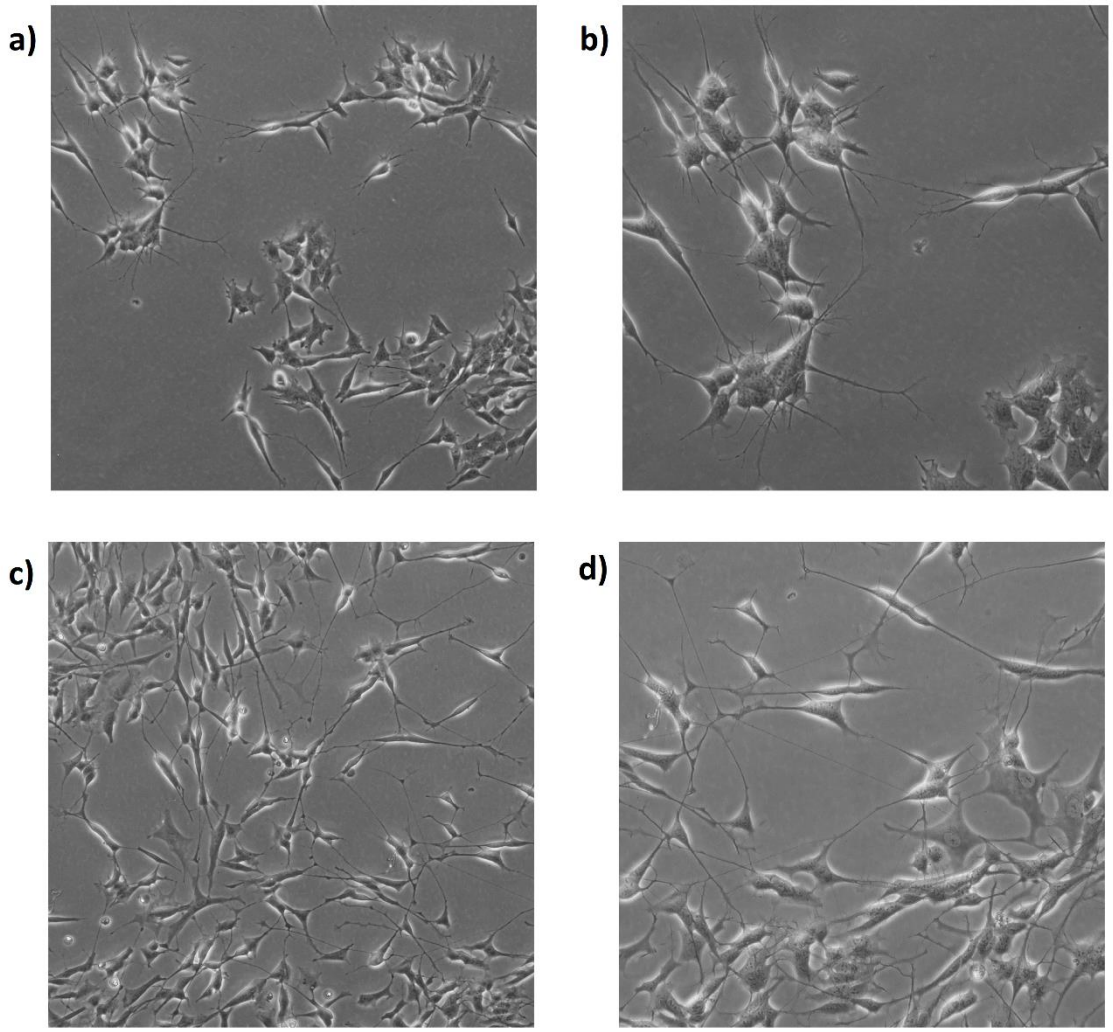

Figure 9: Phase-contrast images of cultured SH-SY5Y cells. a) non-differentiated cells at ×10 magnification; b) non-differentiated cells at ×20 magnification, the cells possess a small number of neurites of a restricted length. c) ATRA treated cells at ×10 magnification; d) ATRA treated cells at ×20 magnification, the cells have elongated extensive neurites forming a network, morphology is altered to be neuron-like; e) synapse-like connections in ATRA treated cells at ×20 magnification.

The genes chosen for the analysis are DLG4 (NMDA receptor-dependent synaptic plasticity mediator), ACHE (terminates the signal at neuron-muscular junctions, involved in neuronal apoptosis(Yang *et al.*, 2002)), NCAM2 (though to be involved in selective fasciculation), SYN1 (coats the synaptic vesicles, binds to the cytoskeleton, thought to mediate the neurotransmitter release), NTNG2 (guides patterning and promotes the neurite elongation (Seiradake *et al.*, 2011)), KCNMA1 (involved in cell membrane depolarisation and cytosolic content of Ca^{2+} regulation, plays a role in neurotransmitter release), GAPDH (involved in glycolysis RNA transport, microtubule assembly, DNA replication and apoptosis control), CDK1 (regulates the cell cycle, promoting G1-S and G2-M transition) (Uniprot). The results of the RT-qPCR with the fluorescence threshold set for 2 show the increase in the expression of DLG4, ACHE, NCAM2 and SYN1 genes; expression of NTNG2, KCNMA1 and CDK1 has decreased (Fig.10). However, only results obtained for ACHE, NCAM2, NTNG2 and CDK1 bear statistical significance.

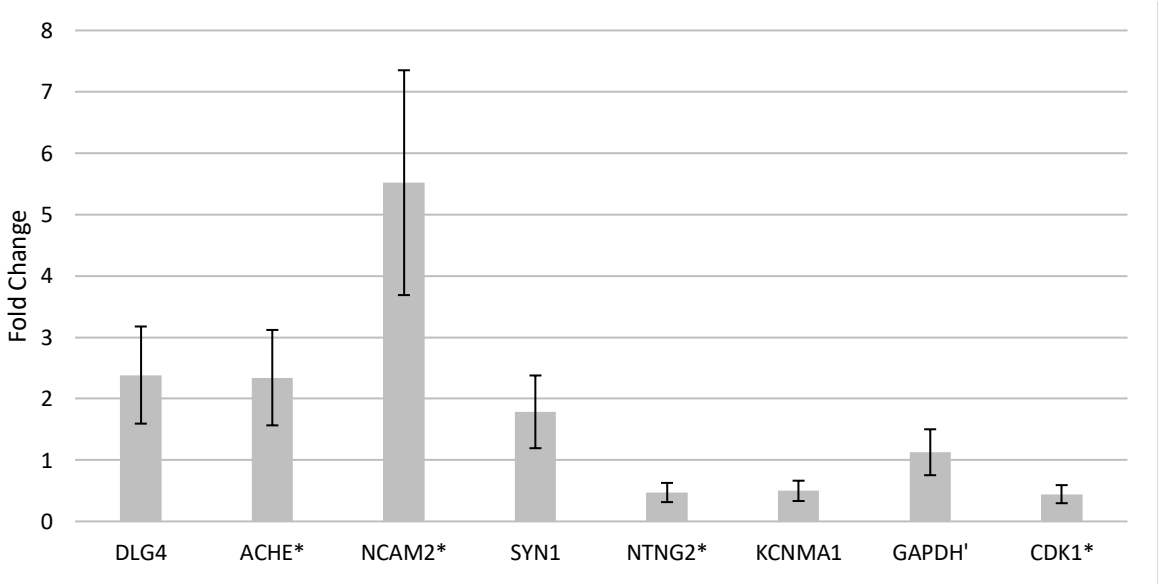

Figure 10: Fold change in the rate of gene expression, statistically significant entries are marked with asterisks, reference housekeeping gene is marked with an apostrophe.

3.2.8 RA Stability has a Minor Effect on the Cell Differentiation

RA is known to be sensitive to temperatures, humidity and light. A 5 fold reduction in the concentration of ATRA in the growth medium upon cell culturing has been reported (Sharow *et al.*, 2012). Intending to improve our culturing protocol, we have tested multiple additions of ATRA to the medium. Fresh ATRA was added to the medium to the f.c. of 15 μM, assuming that the initial concentration of ATRA is 0. Cells with the multiple additions of ATRA during 5 days incubation period do not show any morphological differences

compared to the cells with a single addition of ATRA, and both treatments result in the same decrease of cell proliferation rate (Fig.11).

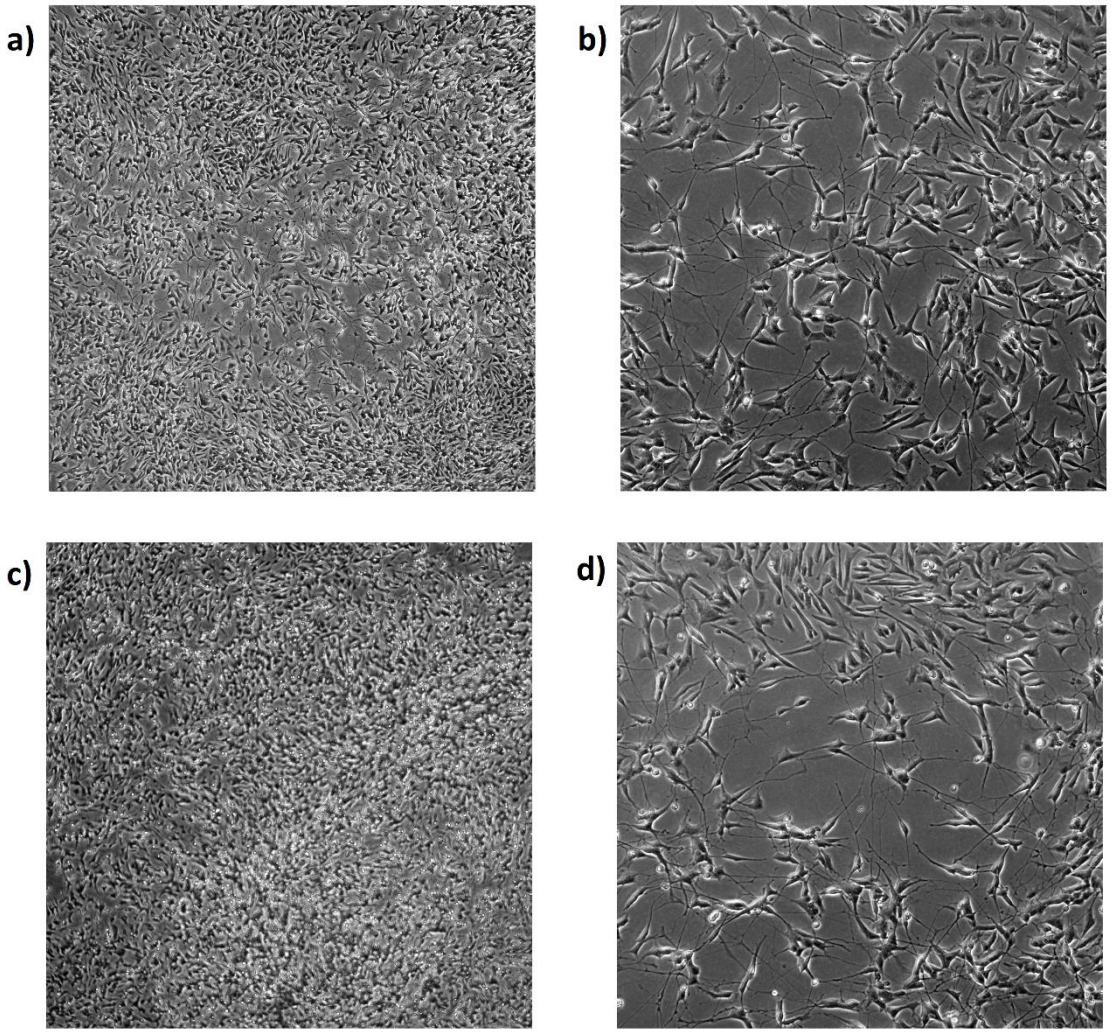

Figure 11: Phase-contrast images of SH-SY5Y cells with multiple ATRA and single addition are compared. a) ATRA added to the cells multiple times, ×4 magnification; b) ATRA added to the cells multiple times, ×20 magnification, the cells possess a small number of neurites of a restricted length. c) ATRA added to the cells once, ×4 magnification; d) ATRA added to the cells once, ×20 magnification.

3.2.9 Transport RNA Granules Derived from SHSY-5Y Contain Key RBPs Characteristic for Transport RNA Granules Derived from Rat Cortical Material

To compare the composition of the SH-SY5Y-derived RNA granules to the transport RNA granules from rat cerebral cortex, we performed a western blot analysis for the presence of key RBPs known to be components of neuronal transport RNA granules: We aimed to detect

three key RBPs known to be an integral part of RNAg's: G3BP-1, G3BP-2 and Caprin-1. Moreover, as transport RNA granules are known to contain large ribosomal subunits (Anderson and Kedersha, 2006), we sought to detect RPL7a, a protein of 60S ribosomal subunit with the molecular weight of 30 kDa (Uniprot). G3BP-1 and G3BP-2 proteins are involved in the process of SG formation by assembling into multimers (Matsuki *et al.*, 2013). G3BP-1 has a molecular weight of 52 kDa and G3BP-2 – 54 kDa (Uniprot). CAPRIN-1 is a protein crucial for the dendritic mRNA transport and long-term memory formation, which is an integral part of transport RNA granules (Nakayama *et al.*, 2017). The molecular weight of CAPRIN-1 is 78 kDa.

The results of the western blot are shown below (Fig.12). FLAG purified fraction does not have a significant amount of detected proteins due to the limited volume of the sample. For the western blot, the FLAG purified sample was diluted and had only 0.003 U of A_{260} in the lane.

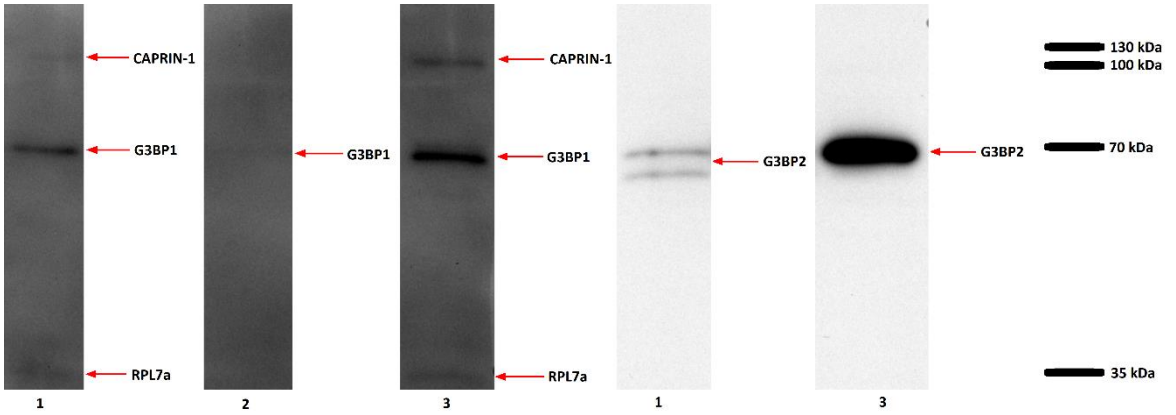

Figure 12: Western blot analysis of RNAg sample purified from neuroblastoma or rat cortex. Lane 1 marks the SHSY-5Y derived non-purified sample; 2 – SHSY-5Y derived, FLX purified; 3 – rat cortical material derived sample.

3.2.10 HHT Treatment of the Cells Prevents the Formation of Polysomes

During the research, the polysomal contamination of the purified transport RNA granule preparation was faced. Therefore, we have tested the effect of the translation inhibitor homoharringtonine (HHT) on the level of polyribosomes in ATRA-differentiated SH-SY5Y. HHT is known to prevent the translocation of the newly assembled 80S ribosome from the start codon, leaving the downstream ribosomes intact (Graber *et al.*, 2013). Thus, it leads to the gradual depletion of actively translating polysomes. However, as transport RNA granules are translationally inactive, HHT treatment leaves them intact, resulting in an enrichment of the preparations for RNA granules over polysomes. To investigate the effect of HHT on the

polysome level in ATRA differentiated SH-SY5Y, we have analysed the polysomal profile of HHT treated cells in a 10-50% sucrose gradient. As controls, we used cells treated with CHX and mock-treated with DMSO. CHX is a translation inhibitor that blocks ribosomal translocation and thus stabilises mRNA-bound ribosomes in a polyribosome (Stanners, 1966). Polysomal profiling showed that HHT tends to decrease the amount of polysomes as there is no sharp peak except for the one corresponding to monosomes. Contrary, CHX treated sample analysis resulted in several distinguishable peaks that show the presence of mono-pentasomes. The non-treated sample contains mRNA bound to four (tetrasome) and five (pentasome) ribosomes (Fig. 13).

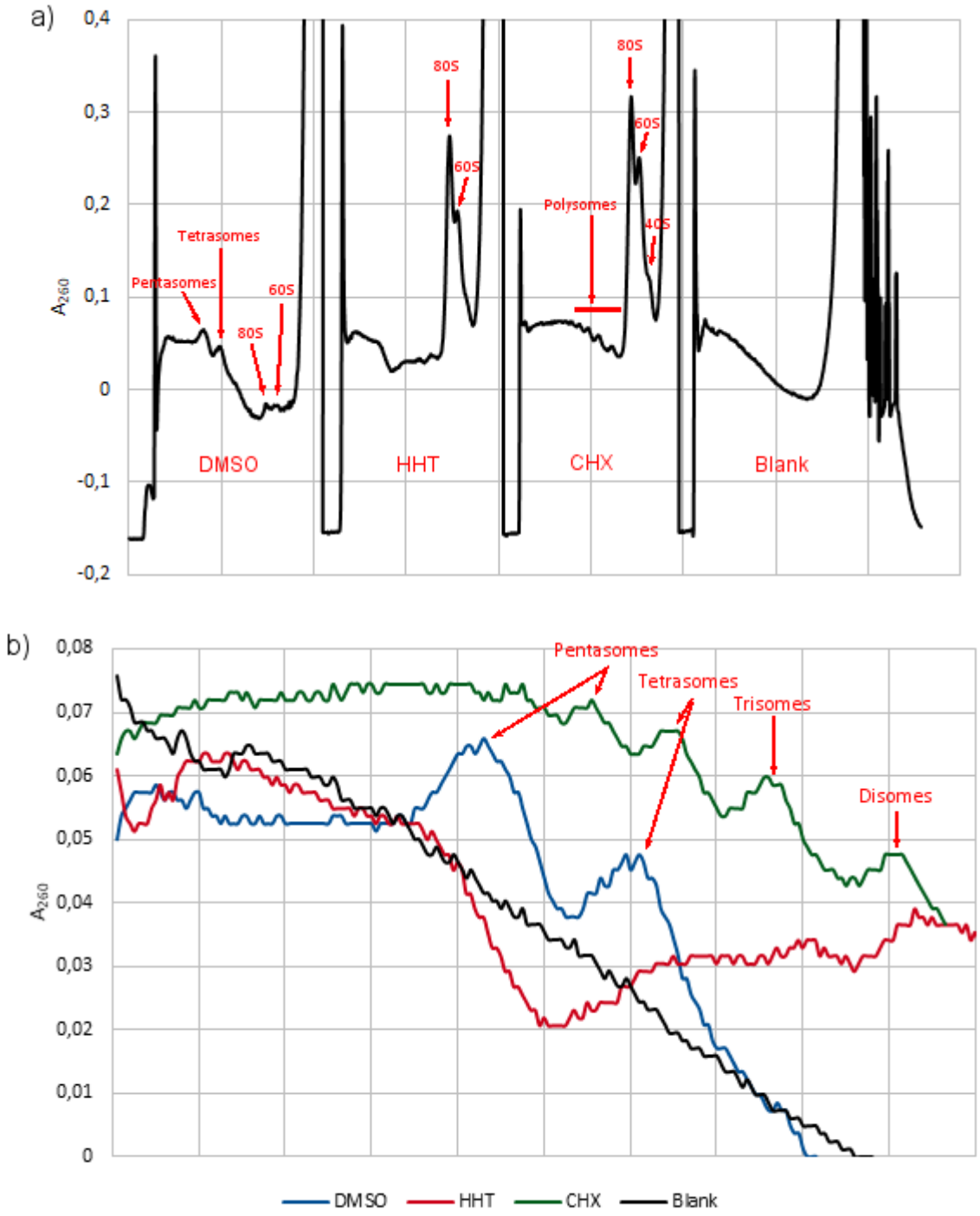

Figure 13: Polysome profiling results are plotted; a) Full polysomal profiling of the samples in the following order: DMSO mock treated, HHT-treated, CHX-treated, pure sucrose gradient; b) "zoomed" profiles of each component: DMSO, HHT and CHX refer to the samples with DMSO mock treatment and HHT and CHX treatment correspondingly. Pure sucrose gradient with no sample was used as a reference and marked "Blank" on the graph

3.3 DISCUSSION

Observed glycogen deposition was expected as the levels of glycogen are upregulated in various cancers: breast, kidney, uterus, bladder, ovary, skin and brain cancer cell lines (Zois *et al.*, 2014). Thus, it is challengeable to reduce the glycogen contamination of the transport RNA granule preparation at the stage of cell culturing. This statement is supported by the result of our insulin experiment. Deprivation of the cells from insulin resulted in the slowed-down proliferation rate as was expected. However, the glycogen contamination of extracted transport RNA granules did not decrease.

Therefore, we have tested different techniques to purify our transport RNA granule preparation from glycogen. α-Amylase treatment did not degrade glycogen in the crude preparation sufficiently. We think the most likely reason for the inability of α-amylase to efficiently degrade the glycogen particles in our transport RNA granule preparation was the short incubation time (30 min) and reduced temperature (RT), as the temperature optimum of α-amylase is close to 37°C. However, incubation of the transport RNA granule preparation at 37°C and prolonged time is not compatible with the structural integrity of the transport RNA granules outside of the cellular milieu, given especially the possibility of the presence of trace amounts of RNase contamination in the commercial α-amylase preparations. Controversial result for the maltose-binding protein affinity chromatography can be explained by the difference in starting amount of material. We suggest that MBP coated resin (Ni-resin) has a certain binding capacity which limits the amount of glycogen extracted. Besides, Ni-resin was reported to bind poly(A)-RNA which are the components of transport RNA granules (Nastasijevic *et al.*, 2008). For this reason, we have decided to abandon the use of MBP for binding the glycogen as a significant number of transport RNA granules can be lost during this purification. FLAG-affinity purification appeared to be at least as efficient technique as MBP Ni-Sepharose despite the initial glycogen content. However, as FLX protein binds RNA non-specifically, the final preparation contains polysomes.

One of the possible reasons for the presence of increased amounts of polysomes in the final transport RNA granules preparation can be the unfolding of the transport RNA granules. Transport RNA granules become translationally active after RBP dissociation and disassemble upon cell depolarisation (Krichevsky and Kosik, 2001). During the culturing, the cells were grown overconfluent, and the growth medium pH shifted from neutral to acidic. Protons present in even slightly acidic medium are capable of interaction with K+ channels,

depolarising the cell (Krishtal and Pidoplichko, 1981). Thus, overconfluency of the cells may cause the disassembly of transport RNA granules by synaptic depolarisation.

Also, FLX could preferably bind to polysomes and enrich these, whereas RNA in transport RNA granules is more protected and not as well accessible to FLX (Nastasijevic *et al.*, 2008). Hence, we have tested the HHT treatment of the cells before the lysis to decrease the number of polysomes. HHT enters the A-site of the ribosome preventing the first round of elongation but not disrupting the assembled polyribosomes (Gandhi *et al.*, 2014). We have successfully proven the efficiency of the prevention of polysomal assembly by HHT with our polysomal profiling experiment (Fig.13). HHT treatment is a promising technique to decrease the number of polysomes in the final preparation, and further research on its possible implementation in the regular culturing process is of major interest.

SHSY-5Y treatment with ATRA alone sufficiently creates neuron-like cells with an extensive network of elongated neurites forming connections morphologically similar to synaptic. This observation goes in accordance with the earlier reposted presence of functional synapses in differentiated neuroblastoma cells (Adem *et al.*, 1987). Moreover, increased rate of expression of synaptic associated genes such as SYN1 and DLG4, despite not having statistical significance in our study, has comparable fold change in previous research (Forster *et al.*, 2016). Compared to the results obtained by the Forster group, we report lower fold change in the expression of ACHE gene. We suggest that the difference might be due to the variation between our protocols of SHSY-5Y ATRA treatment. Forster group has carried out differentiation in two steps: in the first step ATRA was added to the DMEM medium, and only in the second step the DMEM medium was replaced with Neurobasal medium supplemented with ATRA. In addition to ATRA, BDNF was added to the final growth medium further inducing the differentiation of neuroblastoma cells. Moreover, retinyl acetate is present in commercial B27 supplement that is used to prepare “full” neurobasal medium. This compound is approximately 1000 times less effective in the induction of the differentiation than RA, but it is capable of differentiation to some extent (Breitman *et al.*, 1980). Thus, the fold change can be lower as our negative control might be differentiated to a certain degree by the medium itself.

Besides, our RT-qPCR analysis shows the increase in the expression of NCAM2 gene and a decrease in CDK1 and NTNG2 upon cell differentiation. Enhanced expression of NCAM2 was earlier reported to occur in differentiated SH-SY5Y (Korecka *et al.*, 2013). The fold change we observe is slightly lower than reported previously: 5.5-fold compared to 8-fold.

The difference between the observations can result from the periods of ATRA treatment (5 days in our study, and 8 days in the research of Korecka group). Suppression of CDK1 expression is going in line with its function as a key activator of mitosis. At the entrance to the M phase of the cell cycle, CDK1 activity triggers nuclear envelope breakdown, centrosome separation, Golgi fragmentation, assembly of the mitotic spindle and chromosome concentration (Nigg, 2001). Thus, the decrease in the rate of CDK1 expression delays the mitosis, prolonging the interphase and slowing the rate of cell proliferation. Contrary, as NTNG2 promotes neural circuit development, patterning and neurite extension (Seiradake *et al.*, 2011), it was unexpected to see the decrease in its expression upon ATRA differentiation. However, recently published paper by Wenjun Hao suggests the direct participation of netrin protein family in oncogenesis in thyroid, lungs and colon. Therefore, NTNG2 expression is upregulated in cancer cells and promoted by MYC (Wenjun Hao *et al.*, 2020). Previously, ATRA has been shown to suppress MYC expression (Kalemkerian *et al.*, 1994). Hence, we imply that ATRA differentiation may decrease expression of NTNG2 gene via repression of MYC, which can be the reason behind the result obtained by RT-qPCR.

Decomposition of ATRA upon light, temperature and humidity exposure does not have a significant effect on the process of cell differentiation. Morphology of the cells with a single ATRA addition and multiple additions show no difference. Both sets of cells show the neurite outgrowth, synapse-like formation and decrease in the proliferation rate. As the ATRA differentiation is sometimes performed at concentrations much lower than used in our experiments, such relatively high concentration of ATRA can serve as a precaution for the decomposition of the compound upon culturing of the cells.

We have performed the western blot analysis of our transport RNA granules preparation to examine the presence of key RBPs known to be the part of transport RNA granules extracted from *in vivo* systems. All four chosen RBPs are present in both samples: derived from SH-SY5Y and rat cortical material (Fig.12). Detected RPL7a confirms the presence of transport RNA granules but not SGs or PBs as they do not contain large ribosomal subunits (Anderson and Kedersha, 2006). Transport RNA granule preparation validity is further supported by the comparable content of CAPRIN-1 and G3BP-1 within both samples.

The results of our study suggest that SH-SY5Y is a suitable cell line for the development of *in vitro* source of transport RNA granules for their further research. We report that the treatment of the cells with the ATRA alone differentiates them into neuron-like cells to the extend which is sufficient for the extraction and investigation of transport RNA granules similar to

the ones obtained from *in vivo* systems. Therefore, costly and complicated procedures are not a necessity. Glycogen deposition in SH-SY5Y typical of cancer cells cannot be overcome on the stage of cell culturing as we suggest the mechanism by which ATRA upregulates this process. Thus, we have tested different techniques of the crude transport RNA granule preparation purification. In our experiments, FLAG-affinity purification with the FLX protein as an adaptor has shown the best results in reducing the glycogen content. Nevertheless, purified transport RNA granule preparation contains polysomes. In accordance with previous studies, we report the disruption of polysomal formation upon HHT treatment. Hence, such treatment can be a promising tool to reduce polysomal contamination, but this has to be further investigated. As all the manipulations on SH-SY5Y cells are required to be done in a limited time to reduce the cell death, this leads to the restriction on the number of the cell culture dishes. Such restriction limits the number of the culture dishes and implies the need to grow the cells overconfluent to obtain a sufficient amount of material. Our results suggest that, with monitoring the pH and keeping it neutral, processing overconfluent cultures does not lead to alterations in the composition of transport RNA granules or enhanced formation of SGs.

SUMMARY

In our study, we have successfully optimised the protocol of SH-SY5Y culturing for the highest yield of transport RNA granules. To obtain more material cell cultures are first grown in “full” DMEM medium and then differentiated in “full” neurobasal medium supplemented with 15 μM RA. Multiple additions of ATRA did not alter the degree of differentiation, thus, a single addition is sufficient.

In agreement with previous studies, we have observed an efficient differentiation of SH-SY5Y cell culture into neuron-like cells upon ATRA treatment. Such treatment decreases the proliferation rate and supports extensive neurite outgrowth with the formation of synaptic-like connections (Fig.9). RT-qPCR was performed to investigate the fold difference in the gene expression of differentiated and non-differentiated cells. We report the expected increase in the expression levels of ACHE and NCAM2 and suppression of CDK1 expression. An unforeseen decrease in NTNG2 expression goes in accordance with recent findings of Wenjun Hao group.

We attempted to decrease the glycogen contamination of crude transport RNA granule preparation in different ways. Deprivation of the cells from insulin during culturing did not result in significant glycogen removal, so as the amylase treatment of the transport RNA granule sample. Affinity chromatography was the most efficient way to prevent the prevailing of the glycogen granules in the final preparation. MBP based affinity chromatography shows different degree of purification depending on the initial volume of RNAg preparation, which we connect with the restricted binding capacity of the resin and MBP. Efficient purification was obtained using FLAG affinity purification with FLX protein serving as an adaptor. Nevertheless, the final preparation contained polysomes. To reduce the number of polysomes, we have tested the HHT treatment on the cells. After 40 min of incubation with HHT, polysomal profiling shows a significant decrease of polysomes of higher molecular weight.

Western blot performed to compare the abundance of 4 key proteins (CAPRIN-1, G3BP-1, G3BP-2, RPL7a) in rat brain-derived and SH-SY5Y derived material shows the difference in the amount of the protein but not in the presence of any of them. All four proteins are present in both samples providing the evidence of the similarity in the structures of transport RNA granules that we have obtained in comparison with transport RNA granules from *in vivo* systems.

REFERENCES

1. Adem A, Mattsson ME, Nordberg A, Pahlman S. Muscarinic receptors in human SH-SYSY neuroblastoma cell line: regulation by phorbol ester and retinoic acid. *Brain Res.*, 1987, no. 430, pp. 235-242.
2. Anderson P, Kedersha N. RNA granules. *J Cell Biol*, 2006, vol. 6, no. 172, pp. 803-808.
3. Aulas A, Caron G, Gkogkas CG, Mohamed NV, Destroismaisons L, Sonenberg N, Leclerc N, Parker JA, Vande Velde C. G3BP1 promotes stress-induced RNA granule interactions to preserve polyadenylated mRNA. *J Cell Biol*., 2015, vol. 209, no. 1, pp. 73-84.
4. Batish M, Van den Bogaard P, Kramer FR, Tyagi S. Neuronal mRNAs travel singly into dendrites. *PNAS*, 2012, vol. 109, no. 12, pp. 4645-4650.
5. Bramham CR, Wells DG. Dendridic mRNA: transport, translation and function. *Nat Rev Neurosci*, 2007, vol. 8, no. 10, pp.776-789.
6. Breitman TR, Selonick SE, Collins SJ. Induction of differentiation of the human promyelocytic leukemia cell line (HL-60) by retinoic acid. *PNAS*, 1980, vol. 77, no. 5, pp. 2936-2940.
7. Busschots S, O'Toole S, O'Leary JJ, Stordal B. Non-invasive and non-destructive measurements of confluence in cultured adherent cell lines. *MethodsX*, 2015, vol. 2, pp. 8-13.
8. Cajigas IJ, Tushev G, Will TJ, Tom Dieck S, Fuerst N,Schuman EM. The Local Transcriptome in the Synaptic Neuropil Revealed by Deep Sequencing and High-Resolution Imaging. *Neuron*, 2012, vol. 3, no. 74.
9. Castaño Z, Kypta R. Housekeeping Proteins: Limitations as References During Neuronal Differentiation. *The Open Neuroscience Journal*., 2008, no. 2, pp. 36-40.
10. Cheng KW, Agarwal R, Mitra S, Lee JS, Carey M, Gray JW, Mills GB. Rab25 increases cellular ATP and glycogen stores protecting cancer cells from bioenergetic stress. *EMBO Mol Med*., 2012, vol. 4, no. 2, pp. 125-41.
11. Coimbra A. Evaluation of the glycogenolytic effect of alpha-amylase using radioautography and electron microscopy. *J. Histochem Cytochem.*, 1966, vol. 14, no. 12, pp. 898-906.

12. Darnell JC, Van Driesche SJ, Zhang C, Hung KY, Mele A, Fraser CE, Stone EF, Chen C, Fak JJ, Chi SW, Licatalosi DD, Richter JD, Darnell RB. FMRP stalls ribosomal translocation on mRNAs linked to synaptic function and autism. *Cell*, 2011, vol. 146, no. 2, pp. 247–261.
13. Dever TE, Dinman JD, Green R. Translation Elongation and Recoding in Eukaryotes. *Cold Spring Hard Perspect Biol*, 2018, vol. 8, no 10.
14. Dever TE, Green R. The Elongation, Termination, and Recycling Phases of Translation in Eukaryotes. *Cold Spring Hard Perspect Biol*, 2012, vol. 7, no 4.
15. Di Liegro CM, Schiera G, Di Liegro I. Regulation of mRNA transport, localization and translation in the nervous system of mammals (Review). *Int J Mol Med*., 2014, vol. 4, no. 33, pp. 747–762.
16. Duester G. Retinoic acid synthesis and signaling during early organogenesis. *Cell*., 2008, vol. 134, no. 6, pp. 921-931
17. Fatimy R, Davidovic L, Tremblay S, Jaglin X, Dury A, Robert C, De Koninck P, Khandjian EW. Tracking the Fragile X Mental Retardation Protein in a Highly Ordered Neuronal RiboNucleoParticles Population: A Link between Stalled Polyribosomes and RNA Granules. *PLoS Genet*, 2016, vol. 7, no. 12.
18. Forster JI, Köglsberger S, Trefois C, Boyd O, Baumuratov AS, Buck L, Balling R, Antony PM. Characterization of Differentiated SH-SY5Y as Neuronal Screening Model Reveals Increased Oxidative Vulnerability. *J Biomol Screen*., 2016, vol. 21, no. 5, pp. 496-509
19. Furuichi Y, La Fiandra A, Shatkin A. 5′-Terminal structure and mRNA stability. *Nature*, 1977, no. 266, pp. 235–239.
20. Gandhi V, Plunkett W, Cortes JE. Omacetaxine: a protein translation inhibitor for treatment of chronic myelogenous leukemia. *Clin Cancer Res*., 2014, vol. 20, no. 7, pp. 1735-1740.
21. Graber TE, Freemantle E, Anadolu MN, Hébert-Seropian S, MacAdam RL, Shin U, Hoang HD, Alain T, Lacaille JC, Sossin WS. UPF1 Governs Synaptic Plasticity through Association with a STAU2 RNA Granule. *J Neurosci*, 2017, vol. 37, no. 38, pp. 9116–9131.
22. Graber TE, Hébert-Seropian S, Khoutorsky A, David A, Yewdell JW, Lacaille JC, Sossin WS. Reactivation of stalled polyribosomes in synaptic plasticity. *Proc Nati Acad Sci USA*, 2013, vol. 110, no. 40, pp. 16205–16210.

23. Hao W, Yu M, Lin J, Liu B, Xing H, Yang J, Sun D, Chen F, Jiang M, Tang C, Zhang X, Zhao Y, Zhu Y. The pan-cancer landscape of netrin family reveals potential oncogenic biomarkers. *Scientific Reports*, 2020, vol. 10.
24. Hopp TP, Prickett KS, Price VL, Libby RT, March CJ, Cerretti DP, Urdal DL, Conlon PJ. A Short Polypeptide Marker Sequence Useful for Recombinant Protein Identification and Purification. *Bio/Technology*, 1988, vol. 6, no. 10, pp
25. Hörmann H, Gollwitzer R. Bestimmung von Hexosen in Tryptophan-haltigen Eiweisskörpern. Die Kohlenhydratkomponente des Eialbumins. *Justus Liebigs Annalen Der Chemie*, 1962, vol. 655, no. 1, pp. 178–188.
26. Jackson RJ, Hellen CU, Pestova TV. The Mechanism of Eukaryotic Translation Initiation and Prinsiples of its Regulation. *Nat Rev Mol Cell Biol*, 2010, vol. 2, no. 11, pp. 113–127.
27. Jämsä A, Hasslund K, Cowburn RF, Bäckström A, Vasänge M. The retinoic acid and brain-derived neurotrophic factor differentiated SH-SY5Y cell line as a model for Alzheimer's disease-like tau phosphorylation. *Biochemical and Biophysical Research Communications*, 2004, vol. 319, no. 3, pp. 993-1000.
28. Kalemkerian GP, Jasti RK, Celano P, Nelkin BD, Mabry M. All-trans-retinoic acid alters myc gene expression and inhibits *in vitro* progression in small cell lung cancer. *Cell Growth Differ.*, 1994, vol. 5, no. 1, pp. 55-60
29. Kiebler MA, Bassell GJ. Neuronal RNA Granules: Movers and Makers. *Neuron*, 2006, vol. 6, no. 51, pp. 685-690.
30. Korecka JA, Van Kesteren RE, Blaas E, Spitzer SO, Kamstra JH, Smit AB, Swaab DF, Verhaagen J, Bossers K. Phenotypic characterization of retinoic acid differentiated SH-SY5Y cells by transcriptional profiling. *PloS one*, 2013, vol. 8m no. 5.
31. Kovalevich J, Langford D. Considerations for the use of SH-SY5Y neuroblastoma cells in neurobiology. *Methods Mol Biol*., 2013, no. 1078, pp. 9–21.
32. Krichevsky AM, Kosik KS. Neuronal RNA granules: a link between RNA localization and stimulation-dependent translation. *Neuron.*, 2001, vol. 32, no. 4, pp.683-696.
33. Krishtal OA, Pidoplichko VI. Receptor for protons in the membrane of sensory neurons. *Brain Res.*, 1981, vol. 214, no. 1, pp. 150-154.

34. Laver JD, Ly J, Winn AK, Karaiskakis A, Lin S, Nie K, Benic G, Jaberi-Lashkari N, Cao WX, Khademi A, Westwood JT, Sidhu SS, Morris Q, Angers S, Smibert CA, Lipshitz HD. The RNA-Binding Protein Rasputin/G3BP Enhances the Stability and Translation of Its Target mRNAs. *Cell Rep*., 2020, vol. 30, no. 10, pp. 3353-3367.
35. Lewis JD, Izaurralde E. The role of the cap structure in RNA processing and nuclear export. *Eur J Biochem.*, 1997, vol. 247, no. 2, pp. 461-469.
36. Lodish H, Berck A, Kaiser CA, Krieger M, Scott MP, Bretscher A, Ploegh H, Matsudatia P. Molecular Cell Biology 6th Edition. *W.H. Freeman and Co*, 2008, pp. 132-139.
37. López-Carballo G, Moreno L, Masiá S, Pérez P, Barettino D. Activation of the phosphatidylinositol 3-kinase/Akt signaling pathway by retinoic acid is required for neural differentiation of SH-SY5Y human neuroblastoma cells. *J Biol Chem*., 2002, vol. 277, no. 28, pp. 25297-25304.
38. Martin KC, Ephrussi A. mRNA localization: gene expression in the spatial dimension. *Cell*., 2009, vol. 4, no. 136, pp. 719–730.
39. Matsuki H, Takahashi M, Higuchi M, Makokha GN, Oie M, Fujii M. Both G3BP1 and G3BP2 contribute to stress granule formation. *Genes to Cells*, 2013, vol. 18, no. 2, pp. 135-146.
40. Muhič M, Vardjan N, Chowdhury HH, Zorec R, Kreft M. Insulin and Insulin-like Growth Factor 1 (IGF-1) Modulate Cytoplasmic Glucose and Glycogen Levels but Not Glucose Transport across the Membrane in Astrocytes. *J Biol Chem*., 2015, vol. 290, no. 17, pp. 11167-11176
41. Nakayama K, Ohashi R, Shinoda Y, Yamazaki M, Abe M, Fujikawa A, Shigenobu S, Futatsugi A, Noda M, Mikoshiba K, Furuichi T, Sakimura K, Shiina N. RNG105/caprin1, an RNA granule protein for dendritic mRNA localization, is essential for long-term memory formation. *Elife*., 2017, vol. 6, e29677.
42. Nastasijevic B, Becker NA, Wurster SE, Maher LJ 3rd. Sequence-specific binding of DNA and RNA to immobilized Nickel ions. *Biochem Biophys Res Commun*. 2008, vol. 366, no. 2, pp. 420-425
43. Nigg EA. Mitotic kinases as regulators of cell division and its checkpoints. *Nat. Rev. Mol. Cell Biol.*, 2001, vol. 2, pp. 21-32.

44. Ostroff LE, Botsford B, Gindina S, Cowansage KK, LeDoux JE, Klann E, Hoeffer C. Accumulation of Polyribosomes in Dendritic Spine Heads, But Not Bases and Necks, during Memory Consolidation Depends on Cap-Dependent Translation Initiation. *J Neurosci*, 2017, vol. 37, no. 7, pp.1862–1872.
45. Panas MD, Ivanov P, Anderson P. Mechanistic insights into mammalian stress granule dynamics. *J Cell Biol*, 2016, vol. 3, no. 215, pp. 313-323.
46. Ravanidis S, Kattan FG, Doxakis E. Unraveling the Pathways to Neuronal Homeostasis and Disease: Mechanistic Insights into the Role of RNA-Binding Proteins and Associated Factors. *Int. J. Mol. Sci*., 2018, vol. 8, no. 19.
47. Sahoo PK, Lee SJ, Jaiswal PB, Alber S, Kar AN, Miller-Randolph S, Taylor EE, Smith T, Singh B, Ho TS, Urisman A, Chand S, Pena EA, Burlingame AL, Woolf CJ, Fainzilber M, English AW, Twiss JL. Axonal G3BP1 stress granule protein limits axonal mRNA translation and nerve regeneration. *Nat Commun*., 2018, vol. 9, no. 1
48. Seiradake E, Coles CH, Perestenko PV, Harlos K, McIlhinney RA, Aricescu AR, Jones EY. Structural basis for cell surface patterning through NetrinG-NGL interactions. *EMBO J*., 2011, vol. 30, no. 21, pp. 4479-88.
49. Sharow KA, Temkin B, Asson-Batres MA. Retinoic acid stability in stem cell cultures. *Int J Dev Biol.*, 2012, vol. 56, no. 6, pp. 273-278.
50. Shipley MM, Mangold CA, Szpara ML. Differentiation of the SH-SY5Y Human Neuroblastoma Cell Line. *J Vis Exp*., 2016, vol. 108, no. 53193.
51. Stanners SP. The effect of cycloheximide on polyribosomes from hamster cells. *Biochemical and Biophysical Research Communications*, 1966, vol. 24, no. 5, pp. 758-764
52. Sullivan MA, Vilaplana F, Cave RA, Stapleton D, Gray-Weale AA, Gilbert RG. Nature of alpha and beta particles in glycogen using molecular size distributions. *Biomacromolecules*, 2010, vol. 11, no. 4, pp. 1094-1100.
53. Walker IH, Hsieh PC, Riggs PD. Mutations in maltose-binding protein that alter affinity and solubility properties. *Appl Microbiol Biotechnol*., 2010, vol. 88, no. 1, pp. 187-197.
54. Yang L, He HY, Zhang XJ. Increased expression of intranuclear AchE involved in apoptosis of SK-N-SH cells. *Neurosci. Res.*, 2002, vol. 42, no. 4, pp. 261-268.
55. Zois CE, Favaro E, Harris AL. Glycogen metabolism in cancer. *Biochem Pharmacol,*. 2014, vol. 92, no. 1, pp. 3-11.

NON-EXCLUSIVE LICENCE TO REPRODUCE THESIS AND MAKE THESIS PUBLIC

I,

Artur Astapenka,

(*author's name*)

1. herewith grant the University of Tartu a free permit (non-exclusive licence) to

reproduce, for the purpose of preservation, including for adding to the DSpace digital archives until the expiry of the term of copyright,

RNA Granules in Human Neuroblastoma Cell Line SH-SY5Y,

(*title of thesis*)

supervised by Dr Kalle Kipper and Dr Arto Pulk.

(*supervisor's name*)

2. I grant the University of Tartu a permit to make the work specified in p. 1 available to the public via the web environment of the University of Tartu, including via the DSpace digital archives, under the Creative Commons licence CC BY NC ND 3.0, which allows, by giving appropriate credit to the author, to reproduce, distribute the work and communicate it to the public, and prohibits the creation of derivative works and any commercial use of the work until the expiry of the term of copyright.

3. I am aware of the fact that the author retains the rights specified in p. 1 and 2.

4. I certify that granting the non-exclusive licence does not infringe other persons' intellectual property rights or rights arising from the personal data protection legislation.

Artur Astapenka

20/05/2020